Catena 231 (2023) 107274

Contents lists available at ScienceDirect

Catena

journal homepage: www.elsevier.com/locate/catena

Incorporating biotic phosphorus-acquisition strategies into soil phosphorus transformation under long-term salinization in a tidal wetland

Tianning Fan [a,b], Min Luo [a,b,*], Ji Tan [a,c,d], Dehong Hu [a,b], Xin Chen [a,b], Jiafang Huang [a,c,d], Shihua Li [e], Pingping Guo [f], Ji Chen [g,h,i,**]

[a] Research Center of Geography and Ecological Environment, Fuzhou University, Fuzhou 350108, China
[b] College of Environment and Safety Engineering, Fuzhou University, Fuzhou 350108, China
[c] Key Laboratory of Humid Subtropical Eco-Geographical Process, Ministry of Education, Fujian Normal University, Fuzhou 350007, China
[d] College of Geography Science, Fujian Normal University, Fuzhou 35007, China
[e] College of Advanced Manufacturing, Fuzhou University, Jinjiang 362251, China
[f] Fujian Minjiang River Estuary Wetland National Nature Reserve Administrative Office, Fuzhou 350200, China
[g] Department of Agroecology, Aarhus University, Tjele 8830, Denmark
[h] State Key Laboratory of Loess and Quaternary Geology, Institute of Earth Environment, Chinese Academy of Sciences, Xi'an 710061, China
[i] iCLIMATE Interdisciplinary Centre for Climate Change, Aarhus University, Roskilde 4000, Denmark

ARTICLE INFO

Keywords:
Phosphorus limitation
Alkaline phosphomonoesterase
Arbuscular mycorrhizal fungi
Soil phosphorus fractions
Salinization
Tidal wetland soils

ABSTRACT

Tidal wetland plants can maintain high primary productivity under salinization, even with low phosphorus (P) availability. However, little is known about how they adapt to salinization-induced ecosystem P limitation over time. We established mesocosms using tidal freshwater wetland soils and the salt-tolerant plant *Cyperus malaccensis* and subjected them to short-term (6 months) and long-term (3.5 years) salinization. Overall, short-term salinization did not change plant or microbial biomass nitrogen/P ratios, whereas long-term salinization increased both, indicating that short-term salinization did not alter ecosystem P limitation, but long-term salinization exacerbated it. Concurrently, short-term salinization reduced the moderately labile inorganic P (Pi) pool, whereas long-term salinization also reduced the hydrolyzable organic P (Po) and primary mineral P pools. During both short- and long-term salinization, moderately labile Pi mobilization exhibited a negative correlation with Fe sulfide concentration and a positive correlation with Fe(III) concentrations. These results suggested that both short- and long-term salinization obtained P through abiotic P-acquisition strategies. Mobilization of the primary mineral P pool and hydrolyzable Po pools was negatively linked to root arbuscular mycorrhizal fungi (AMF) biomass and soil alkaline phosphomonoesterase (ALP) activity, respectively. This indicated that long-term salinization acquired P via biotic P-acquisition strategies. Specifically, soil microorganisms increased fungi predominance and thereby increased ALP activity to convert hydrolyzable Po, while tidal wetland plants enhanced root AMF associations to release carboxylate to transform primary mineral P. Overall, our results highlight that abiotic P-acquisition strategies could offset the ecosystem P limitation during short-term salinization, whereas biotic P-acquisition strategies play a more important role in soil P transformation under long-term salinization. Through biotic P-acquisition, tidal wetland ecosystems can maintain high plant primary productivity through biotic P-acquisition even under P-limited conditions, exhibiting increased resilience to sea-level rise.

1. Introduction

The global sea level has increased at a rate of 3.2–4.2 mm yr^{-1} over recent decades (IPCC, 2022). Such a rapid rise in the sea level leads to transient or sustained salinization in low-lying coastal zones (Neubauer, 2013; Tully et al., 2019). Tidal wetlands are influenced by both

* Corresponding authors at: College of Environment and Safety Engineering, Fuzhou University, Wulongjiang North Avenue Street #2, Minhou County, Fuzhou 350116, China. School of Geographical Science, Fujian Normal University, Xuefu South Road #8, Minhou County, Fuzhou 350117, China.
** Corresponding authors at: Department of Agroecology, Aarhus University, Tjele 8830, Denmark
E-mail addresses: luomin@fzu.edu.cn (M. Luo), ji.chen@agro.au.dk (J. Chen).

https://doi.org/10.1016/j.catena.2023.107274
Received 3 May 2023; Received in revised form 30 May 2023; Accepted 3 June 2023
Available online 12 June 2023
0341-8162/© 2023 The Author(s). Published by Elsevier B.V. This is an open access article under the CC BY license (http://creativecommons.org/licenses/by/4.0/).

astronomical tides and river discharge, which are vulnerable to sea-level rise-induced salinization (Megonigal and Neubauer, 2009; Luo et al., 2019). Indeed, tidal wetland research has shown that salinization affects carbon (C) sequestration and decomposition (Craft, 2007; Więski et al., 2010; Chambers et al., 2013; Neubauer, 2013; Zhao et al., 2018; Servais et al., 2019; Liu et al., 2021), as well as nitrification and nitrogen (N) mineralization (Abell et al., 2013; Zhou et al., 2017). Phosphorus (P) is an important nutrient in tidal wetland ecosystems, which has critical roles for plant growth and development (Więski et al., 2010; Hou et al., 2020). However, compared with the wealth of information on the responses of C and N cycles to salinization (Herbert et al., 2015; Tully et al., 2019), its effects on P cycles in tidal wetland ecosystems are poorly understood.

Tidal wetlands are regarded as the most productive ecosystems on Earth (Neubauer and Craft, 2009; Zhou et al., 2017), despite prevailing ecosystem P limitation (Hou et al., 2020). Salinity is a physiological stressor for plants; thus, plant primary productivity is expected to decline with increasing salinity (Więski et al., 2010; Neubauer, 2013). However, two recent studies showed that salt-tolerant plants in tidal wetlands could maintain high primary productivity under salinization, even though ecosystem P limitation was exacerbated with increasing salinity (Wilson et al., 2019; Zhai et al., 2022). These unexpected findings indicate that tidal wetland plants might have efficient P-acquisition strategies to alleviate ecosystem P limitation (Noe et al., 2012; Wilson et al., 2019). Clarifying the P-acquisition strategies under salinization and exploring their underlying mechanisms are crucial to accurately predict how tidal wetland ecosystems respond to the imminent sea level rise.

Soil P is locked in the form of labile and moderately labile inorganic P (Pi) and organic P (Po), primary mineral P, and occluded P, which can be transformed to available P through both abiotic and biotic processes (Hedley et al., 1982; Tiessen and Moir, 2007). Salinization could influence soil P transformation via abiotic processes in tidal wetland soils (Paludan and Morris, 1999; Jordan et al., 2008; Xu et al., 2012; Jun et al., 2013; Hartzell et al., 2017; Zhao et al., 2019; Hu et al., 2022b). Tidal wetland soils are enriched in ferric iron oxides/hydroxides [Fe (III)] (Kostka et al., 2002; Luo et al., 2019), and most phosphates are bound to Fe(III) (Bai et al., 2017; Jordan et al., 2008). Salinization also elevated the sulfate (SO_4^{2-}) concentrations by 2–5 orders of magnitude in the tidal wetland soils (Lamers et al., 2013; Schoepfer et al., 2014). Therefore, microbial sulfate reduction would prevail in tidal wetland ecosystem after salinization (Neubauer et al., 2013; Chambers et al., 2013; Luo et al., 2020). The process of microbial sulfate reduction is associated with the production of sulfides (Hyun et al., 2007; Kristensen et al., 2011). As excess sulfide is produced, it has the potential to drive the reduction of Fe(III) and yields Fe sulfides (Burton et al., 2006; Keene et al., 2011). This abiotic process could cause the desorption of phosphate bound to Fe(III), further increasing available P concentrations in the soils (Jordan et al., 2008; Jun et al., 2013; Bai et al., 2017). Therefore, the abiotic P-acquisition strategy plays a vital role in soil P transformation under salinization in tidal wetland ecosystems.

It remains unclear whether salinization induces a biotic P-acquisition strategy to regulate the soil P transformation in the tidal wetlands (Noe et al., 2012; Wilson et al., 2019). Generally, biotic P-acquisition strategies involve phosphatase and mycorrhizal fungi (Liu et al., 2021; Hu et al., 2022a). For example, soil microbes and partial plants could release phosphatases, such as acid phosphomonoesterase (ACP) and alkaline phosphomonoesterase (ALP) (Marklein and Houlton, 2012; Luo et al., 2022). These phosphatases can further catalyze the hydrolysis of phosphate ester bonds, which are commonly found in organic P compounds, such as nucleotides, inositol phosphates, and phospholipids (Chen et al., 2019; Hu et al., 2022a). The hydrolysis reaction removes the organic groups attached to the phosphate molecule, releasing phosphate that is readily available for plants and soil microbes (Pant and Warman, 2000; Jarosch et al., 2019). Indeed, several recent studies have reported that phosphatase activity increases with increasing salinity in tidal wetland soils (Servais et al., 2019; Zhai et al., 2022), suggesting that plants and soil microbes in tidal wetland ecosystems have the potential to enhance P-acquisition by increasing phosphatase activity under salinization (Zhai et al., 2022). Additionally, plants in terrestrial ecosystems can increase P mobilization through enhanced associations with mycorrhizal fungi, including ectomycorrhizal fungi (ECF) and arbuscular mycorrhizal fungi (AMF) (Chen et al., 2020; Ding et al., 2021; Liu et al., 2021). ECF associations occur exclusively in trees and shrubs, whereas AMF associations comprise mutualistic symbiosis among 80% of vascular plants (Muthukumar et al., 2004; Xu et al., 2016). Over the last few decades, tidal wetland plants living in freshwater wetlands (Šraj-Kržič et al., 2006; Zhang et al., 2014), salt marshes (Sengupta and Chaudhuri, 1990; Carvalho et al., 2003), and mangrove forests (Wang et al., 2010; Gupta et al., 2016) have been found to be associated with AMF. AMF can secrete organic acids, such as carboxylate, to mobilize P through chelation with metal cations, such as Ca^{2+}, Fe^{3+}, and Al^{3+}, forming soluble complexes (Zhou et al., 2021; Ding et al., 2021; Luo et al., 2022). Additionally, carboxylates can directly compete with P for sorption sites on soil particles, reducing the adsorption of P onto the soil and increasing its mobility (Neumann and Martinoia, 2002; Lambers et al., 2012; Hu et al., 2022a). Therefore, AMF associations might also help host plants to acquire P in tidal wetlands. Overall, tidal wetland ecosystems might stimulate the transformation of soil P through biotic P-acquisition strategies under salinization, though there is a paucity of experimental evidence of this.

The ecosystem P limitation can change over time under salt stress. A few laboratory experiments suggested that ecosystem P limitation is alleviated under salinization in the tidal wetland, since saltwater addition would cause P desorption (Flower et al., 2017; Price et al., 2010). By contrast, studies conducted along the natural salinity gradient of estuarine tidal wetlands showed that plant nitrogen/phosphorus (N/P) ratio, which is a proxy of ecosystem P limitation, increase with salinity (Więski et al., 2010; Zhai et al., 2022). This finding potentially offers insights suggesting that long-term salinization would increase ecosystem P limitation in tidal wetland ecosystems (Morrissey et al., 2014; Zhai et al., 2022). Moreover, a mesocosm experiment showed that P availability increases within the first 7 months, whereas extended saltwater exposure over a period of two years causes a decrease in P availability (Wilson et al., 2019). These results together suggested that ecosystem P limitation might change over time, which could further lead to variations in P-acquisition strategies (Marklein and Houlton, 2012; Chen et al., 2020). However, it remains unclear whether salinization-stimulated biotic and abiotic P-acquisition strategies are persistent or temporally dynamic.

Here, we set up mesocosms with tidal freshwater wetland soils, then planted them with the indigenous salt-tolerant plant *Cyperus malaccensis* Lam., and subsequently subjected them to four salinity treatments. The plant and soil samples were collected under both short- (6 months) and long-term (3.5 years) salinization. We examined soil P fractions, plant N/P ratios, microbial biomass N/P ratios, activities of soil phosphatase, and root AMF biomass. The goal of this study was to explore which P-acquisition strategies are adopted by the tidal wetland ecosystem under salinization and whether these P-acquisition strategies change over time. We hypothesized the following: (I) that ecosystem P limitation will be exacerbated when salinization is extended from the short to long term, probably because of maintaining high plant biomass under long-term salinization; (II) that both short- and long-term salinization will mobilize labile Pi pools through abiotic P-acquisition strategies; and (III) that long-term salinization will also mobilize relatively recalcitrant P pools by stimulating biotic P-acquisition strategies, owing to the acclimation of plants and soil microbes.

2. Materials and methods

2.1. Soil preparation

The soil and plants used in this experiment were collected from a tidal freshwater wetland in the Min River Estuary, southeast China (25°57′0″–25°57′30″N, 119°20′0″–119°22′0″E) (Fig. 1**a and 1b**). The study site is characterized by a typical subtropical oceanic monsoon climate, with a mean annual temperature of 21.1 °C and a mean annual rainfall of 1250 mm (Luo et al., 2020). The site experiences a semi-diurnal tide. Surface tidal wetland soils are classified as Ultisol. The soil salinity level was 0.4 ± 0.2 ppt (part per thousand). The soil texture was silty loam with 36–43% sand, 46–53% silt, and 10–12% clay (Luo et al., 2020). The content of soil organic carbon was 10–30 g kg^{-1}, and the total N content was<3 g kg^{-1} (Zhai et al., 2022). The dominant indigenous plant species at the study site was *C. malaccensis*, which has a high salt tolerance of 0–15 ppt (Liu et al., 2021).

2.2. Experimental design

The salinization experiment was conducted in an indoor simulated tidal system consisting of a salinity treatment tank, tidal reservoir, pump, and inflow and outflow pipes (Fig. 1**d**). The water level was controlled by the pump, which simulated tidal flooding and ebbs twice per day. Four levels of salinization treatments were set up in each simulated tidal system as follows: control (salinity = 0.5 ppt), low-salinity (salinity = 3.0 ppt), mid-salinity (salinity = 6.0 ppt), and high-salinity (salinity = 9.0 ppt) (Fig. 1**c**). The salinity of the control was set according to the soil salinity of the study site, whereas that of low-, mid-, and high-salinity treatments was set according to the level of salinization that could occur in most tidal freshwater wetlands in the coming years, decades, and centuries, respectively (Woodroffe and Murray-Wallace, 2012; Morrissey et al., 2014).

In January 2017, the soils at the study site were collected, pooled, passed through a 2 mm mesh nylon sieve, and transferred to 40 polyvinyl chloride cores (inner diameter = 15 cm; height = 40 cm). Each tidal pool contained 10 polyvinyl chloride cores. All cores were flooded with freshwater for 1 month. On February 15–19, 2017, *C. malaccensis* seedlings of similar lengths (8–12 cm) were collected from the study site and planted in each polyvinyl chloride core at a natural stem density (~500 stem m^{-2}; Liu et al., 2021). Salinization started on February 20, 2017 and ended on August 16, 2020. During the experimental period, half of the cores was harvested after 6 months (August 28, 2017), and the other half was sampled at the end of the experiment, that is, 3.5 years after initiation. In order to avoid the influence of seasons, both sampling times were in summer. According to previous studies, a 3.5-year experiment would be sufficient to detect the effects of salinization on the microbial community composition and plant primary productivity (Dang et al., 2019; Servais et al., 2019; Wilson et al., 2019).

2.3. Plant and soil sampling

During sampling, shoots were clipped and roots were removed from the soil and washed. The fine root samples (diameter, < 0.5 mm) were frozen, freeze-dried, weighed, and ground for root AMF biomass measurements (Hu et al., 2022a). Shoots and roots were oven-dried at 70 °C to a constant weight and then weighed (Drake and Ungar, 1989). The dried plant samples were ground for N and P analyses. Plant N concentrations were measured using a CN elemental analyzer (Elementar Analysensysteme GmbH, Hanau, Germany). Plant P was extracted using a mixture of sulfuric acid and perchloric acid (Sparks, 1996), and the extracted P was determined using a San++ continuous flow analyzer (Skalar Analytical, Breda, Netherlands).

We sampled the 0–10 cm soil-surface layer. This sample depth was

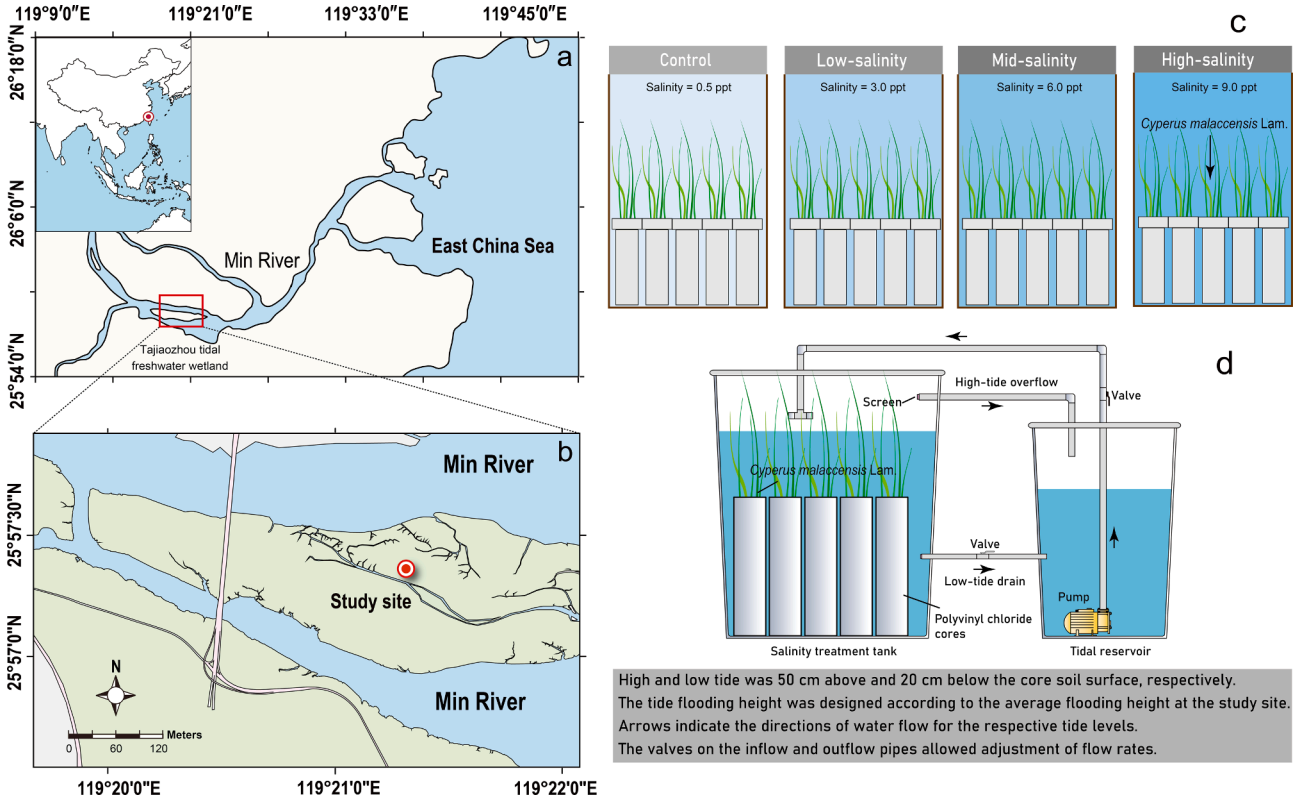


Fig. 1. Location of the study site in the Tajiaozhou tidal freshwater wetland (b) of the Min River Estuary of the East China Sea (a). Schematic illustration of the mesocosm experiment based on tidal freshwater wetland soils subjected to four salinity treatments (c). Schematic illustration of the salinity treatment tank and a tidal reservoir (d).

selected because it was the most affected by overlying tide water in our previous study (Liu et al., 2021). In the laboratory, soil samples were pooled and sieved (mesh size = 2 mm) to remove roots. Soil subsamples for geochemical and microbial determination analyses were stored at 4 and − 20 °C, respectively.

2.4. Soil abiotic property analysis

Soil reactive Fe(II) was extracted using hydrochloric acid, and total reactive Fe was extracted using a mixture of hydrochloric acid and hydroxylamine (Luo et al., 2014). Both reactive Fe(II) and total Fe concentrations were detected through photometric analysis using a UV-2450 spectrophotometer (Shimadzu, Kyoto, Japan). Soil reactive Fe (III) concentrations were calculated as the difference between the total reactive Fe and Fe(II) concentrations. Sulfide [mainly consisting of FeS in the study site (Luo et al., 2015)] was extracted with an acid chromium chloride solution (Hyun et al., 2007), and the extracted S concentration was detected via photometric analysis using a UV-2450 spectrophotometer (Shimadzu). The recovery of Fe(II), Fe(III), and sulfide were assessed using ferrous carbonate, ferric oxide-hydroxide, and sodium sulfide, and were found to be 97%–104%, 96%–102%, and 92%–107%, respectively. The Fe sulfide concentrations were estimated by considering the stoichiometric proportion of Fe and S with a 1:1 ratio (Keene et al., 2011).

The soil P fractions were sequentially extracted using a modified Hedley fractionation procedure (Hedley et al., 1982; Tiessen and Moir, 2007). Briefly, 1.0 g of soil was extracted using an anion-exchange resin membrane strip in deionized water, followed by treatment with 0.5 mol L^{-1} $NaHCO_3$ (pH = 8.5), 0.1 mol L^{-1} NaOH, and 1 mol L^{-1} HCl, followed by hot concentrated HCl. The residual P was digested using concentrated sulfuric acid at 350 °C for 3 h. For $NaHCO_3$, NaOH, and hot HCl extraction, total P was determined using the same method after digestion for 1 h using acid ammonium persulfate in an autoclave. Organic P in $NaHCO_3$, NaOH, and hot HCl extractions was calculated as the difference between the undigested and digested samples. The P concentration in each extract was determined using the San++ continuous flow analyzer (Skalar Analytical). Finally, we obtained resin-Pi, $NaHCO_3$-Pi, $NaHCO_3$-Po, NaOH-Pi, NaOH-Po, HCl-Pi, hot HCl-Pi, hot HCl Po, and residual P. To reflect their ecological importance, the soil P fractions were grouped as follows (Liu et al., 2021; Zhou et al., 2021; Hu et al., 2022a): available P (resin-Pi and $NaHCO_3$-Pi), labile Po ($NaHCO_3$-Po), moderately labile Pi (NaOH-Pi), moderately labile Po (NaOH-Po), primary mineral P (HCl-P), and occluded P (including hot HCl Pi, hot HCl Po, and residual P). The total P concentration was calculated as the sum of the six soil P fractions. The hydrolyzable P was calculated as the sum of labile Po and moderately labile Po.

2.5. Soil microbial activity analysis

Microbial biomass N and P were detected through chloroform fumigation extraction (Brookes et al., 1982). Briefly, one portion of soil (10 g fresh weight soil) was fumigated, while another portion was used as a control. Both fumigated and non-fumigated soil samples were extracted using 0.5 mol L^{-1} potassium sulfate and 0.5 mol L^{-1} sodium bicarbonate solution for microbial biomass N and P, respectively. Microbial biomass N and P were calculated as the difference between fumigated and non-fumigated aliquots at an extraction coefficient of 0.54 and 0.40, respectively. Microbial biomass N and P in each extract were determined using the San++ continuous flow analyzer (Skalar Analytical). The activities of ACP and ALP were assayed using p-nitrophenyl phosphate (PNP) as a substrate at pH 6.5 and 11, respectively (Tabatabai, 1994). Fluorescence was measured using a microplate reader (Synergy H4 Hybrid Multi-Mode, BioTek Instruments Inc., VT, USA).

2.6. Lipid extraction and analysis

The biomass of the bacteria and fungi in soil samples was characterized based on its phospholipid fatty acids (PLFAs), whereas the biomass of AMF in root samples was measured based on its neutral lipid fatty acids (NLFAs) (Frostegård and Bååth, 1996; Olsson et al., 1995). Briefly, the total lipids of freeze-dried soil (3 g) and root (20 mg) subsamples were extracted with a mixture of chloroform, methanol, and citrate buffer at a volume ratio of 1:2:0.8. The lipid extracts were separated into neutral lipids, glycolipids, and phospho-lipids using silica acid columns (Supelco Inc., USA). Both PLFA and NLFA residues, using fatty acid 19:0 as the internal standard, were analyzed using an Agilent 6890 N gas chromatograph (Agilent Technologies, Lexington, MA, USA). Identification was performed using fungal fatty acid standards and MIDI peak identification software (Microbial ID Inc., USA). The PLFAs i14:0, i15:0, a15:0, i16:0, i17:0, a17:0, 16:1ω9c, 16:1ω7c, cy17:0, 18:1ω7c, 18:1ω5c, and cy19:0 were assigned to bacteria, whereas the PLFAs 16:1ω5c, 18:2ω6, 9c, and 18:1ω9c were assigned to fungi (Zhou et al., 2021). The NLFA 16:1ω5c was used as the indicator of AMF (Olsson et al., 1995).

2.7. Data analysis

All analyses were conducted using R software (version 4.1.3; The R Foundation, Vienna, Austria), with a level of statistical significance of $p < 0.05$. All datasets were analyzed for homogeneity and normality, and heterogenous/non-normally distributed data were log_{10}-transformed. Repeated measures ANOVA was used to assess variation due to the salinity effects and time using the "*aov*" function. Tukey's post hoc test was used for multiple comparisons among the four salinity treatments, either within the short- or long-term experiments. Pairwise comparisons between short- and long-term salinization were performed using a paired sample *t*-test. Redundancy analysis (RDA) was used to identify the environmental factors that affected changes in soil P fractions; then, variance partitioning analysis (VPA) was used to determine the relative contributions of biotic and abiotic factors to the regulation of soil P fractions. Both RDA and VPA were used the "*vegan*" package in R. Linear regression models were used to test the relationships among soil P fractions, root AMF biomass, Fe(III) concentrations, Fe sulfide concentrations, and phosphatase activities using the "*lm*" method in R. A structural equation model (SEM) was built using the "*lavaan*" package to explore the impact of salinization on available P. The hypothesized model structure was based on salinity determining available P by influencing biotic (including phosphatase activity and AMF biomass) and abiotic (including Fe sulfide concentrations) factors (**Fig. S1**). The parameters for the final model were selected based on goodness of fit (assessed using a comparative fit index [CFI]), a Akaike Information Criterion (AIC), and a chi-squared test. If CFI was greater than 0.9, the AIC was low, and the chi-square test was non-significant, the model was considered to have a good fit.

3. Results

3.1. Plant properties under salinization

Soil salinity significantly increased from 0.30 to 7.92 ppt among the four treatments during short-term salinization, and from 0.44 to 8.21 ppt during long-term salinization (Table 1). The range of plant P concentrations varied from 1.10 ± 0.06 to 1.39 ± 0.11 g P kg^{-1}, while the range of plant N concentrations varied from 11.27 ± 0.66 to 13.55 ± 1.18 g N kg^{-1} (Fig. 2**a and 2b**). The range of plant N/P ratios varied from 18.17 ± 1.88 to 26.02 ± 2.36 (Fig. 2**c**). Plant P concentrations and plant N/P ratios did not change with increasing salinity during short-term salinization (Fig. 2**a and 2c**). By contrast, plant P concentrations decreased, whereas plant N/P ratios increased, as salinity increased during long-term salinization (Fig. 2**a and 2c**). Lower plant P

Table 1
Changes in soil abiotic properties (mean ± standard deviation, n = 5) after experimental salinization in tidal wetlands of the Min River Estuary, East China Sea.

Time	Treatment	Salinity ppt	Fe(III) μmol Fe g^{-1}	Fe(II) μmol Fe g^{-1}	Fe sulfide μmol Fe g^{-1}
Short-term	**Control**	0.30 ± 0.08 Ad	56.07 ± 7.83 Aa	25.46 ± 4.26 Aa	1.93 ± 0.58 Ac
	Low-salinity	2.21 ± 0.06 Ac	40.56 ± 3.77 Ab	15.01 ± 2.01 Ab	17.74 ± 1.21 Ab
	Mid-salinity	4.92 ± 0.01 Ab	44.63 ± 7.73 Aab	15.14 ± 1.64 Ab	20.56 ± 3.67 Ab
	High-salinity	7.92 ± 0.04 Aa	33.29 ± 8.54 Ab	13.44 ± 1.11 Ab	28.03 ± 1.20 Aa
Long-term	**Control**	0.44 ± 0.05 Ad	53.83 ± 10.74 Aa	26.49 ± 2.61 Aa	0.49 ± 0.26 Ac
	Low-salinity	2.38 ± 0.13 Ac	39.89 ± 2.68 Ab	15.85 ± 2.73 Ab	18.50 ± 3.11 Ab
	Mid-salinity	5.13 ± 0.07 Ab	37.08 ± 3.13 Ab	14.74 ± 3.00 Ab	20.86 ± 5.65 Aab
	High-salinity	8.21 ± 0.09 Aa	31.41 ± 4.02 Ab	13.16 ± 0.81 Ab	26.59 ± 4.97Aa
Source of variation [a]					
Salinity		***	***	***	***
Time		*n.s.*	*n.s.*	*n.s.*	*n.s.*
Salinity × Time		*n.s.*	*n.s.*	*n.s.*	*n.s.*

Capital letters indicate significant differences ($p < 0.05$; *t*-test) between the short- and long-term experiments. Lowercase letters indicate significant differences ($p < 0.05$; Tukey's post hoc test) among the four salinity treatments within either the short- or long-term experiment.
(*n.s.*, not significant; *$p < 0.05$, **$p < 0.01$, and ***$p < 0.001$).
ppt: part per thousand.
[a] The experiment times are as follows: short-term = 6 months and long-term = 3.5 years.

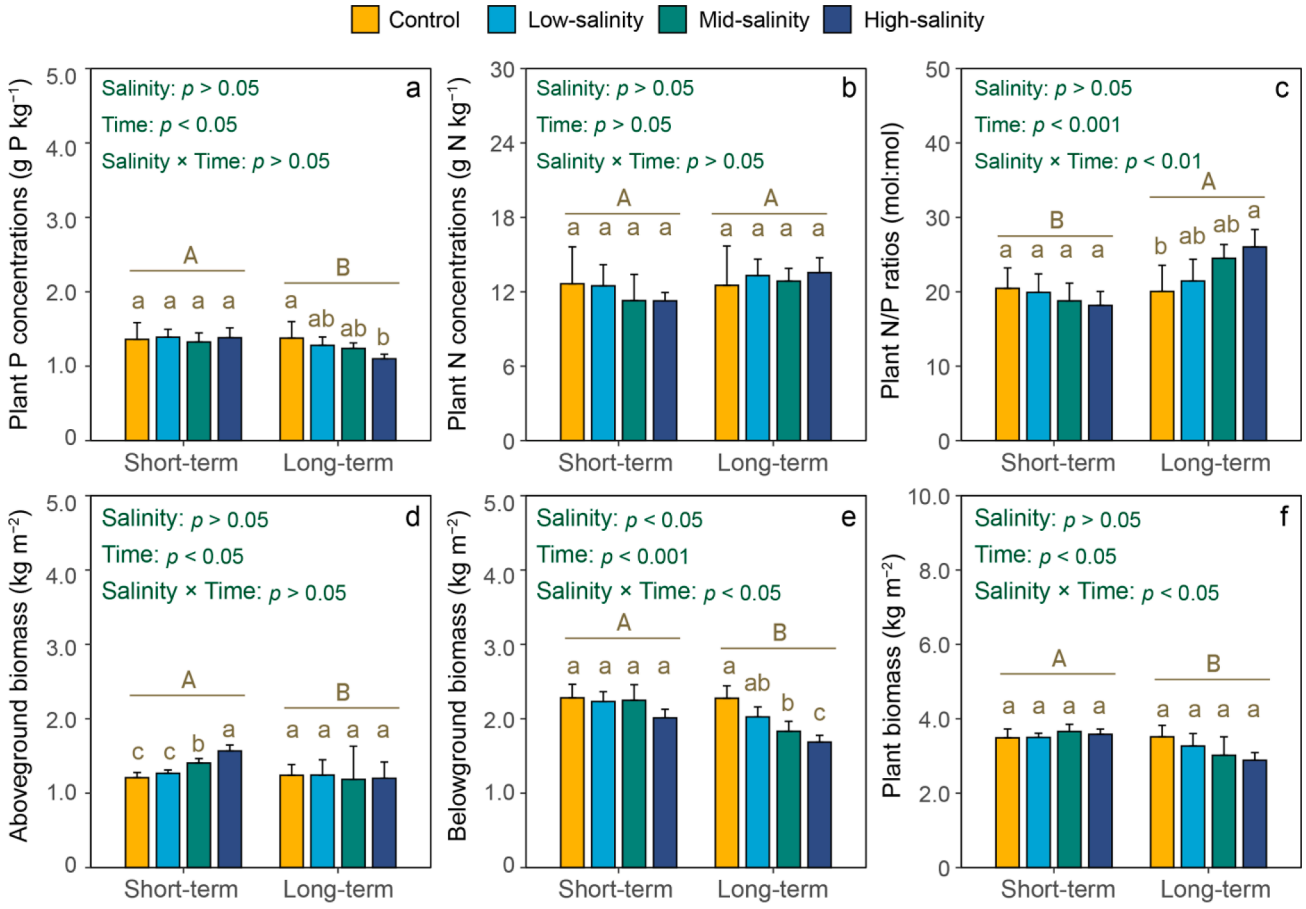


Fig. 2. Changes of plant properties under short- and long-term salinization. Data are presented as the mean ± standard deviation (n = 5). Capital letters indicate significant differences ($p < 0.05$; *t*-test) between the short- and long-term experiments. Lowercase letters indicate significant differences ($p < 0.05$; Tukey's post hoc test) among the four salinity treatments either within the short- or long-term experiment. N/P: nitrogen/phosphorus.

concentrations and higher plant N/P ratios concentrations were observed during long-term salinization compared to those with short-term salinization (Fig. 2**a and 2c**). Both salinity and time did not affect plant N concentrations (Fig. 2**b**). Plant biomass ranged from 2.89 ± 0.20 to 3.66 ± 0.20 kg·m^{-2} (Fig. 2**f**), with aboveground biomass varying from 1.19 ± 0.44 to 1.57 ± 0.08 kg·m^{-2} (Fig. 2**d**) and belowground biomass ranging from 1.69 ± 0.09 to 2.28 ± 0.18 kg·m^{-2} (Fig. 2**e**). Aboveground biomass increased with increasing salinity during short-term salinization but did not change as salinity increased during long-term salinization (Fig. 2**d**). In comparison, belowground biomass did not change with increasing salinity during short-term salinization but decreased as salinity increased during long-term salinization (Fig. 2**e**). Both salinity and time did not affect total plant biomass (Fig. 2**f**).

3.2. Soil microbial properties under salinization

The range of microbial biomass P varied from 22.53 ± 1.33 to 38.96 ± 3.15 mg P kg^{-1}, while the range of microbial biomass N varied from 56.34 ± 11.13 to 64.62 ± 16.98 mg N kg^{-1} (Fig. 3**a and 3b**). The range of microbial biomass N/P ratios varied from 3.33 ± 0.77 to 6.16 ± 0.94 (Fig. 3**c**). Microbial biomass P and microbial biomass N/P did not change among the salinity treatment groups during short-term salinization (Fig. 3**a and 3c**). In contrast, microbial biomass P decreased, whereas microbial biomass N/P increased with increasing salinity during long-term salinization. Both salinity and time did not affect microbial biomass N (Fig. 3**b**).

The range of fungal biomass varied from 1.31 ± 0.19 to 2.68 ± 0.23 nmol PLFA g^{-1} soil, while the range of bacterial biomass varied from 17.07 ± 0.62 to 22.17 ± 6.61 nmol PLFA g^{-1} soil (Fig. 3**d and 3e**). The range of fungi/bacterial ratios varied from 0.06 ± 0.01 to 0.16 ± 0.04 (Fig. 3**f**). The range of root AMF biomass varied from 0.84 ± 0.15 to 1.60 ± 0.14 nmol NLFA g^{-1} root (Fig. 3**g**). The range of soil ACP activity varied from 4.98 ± 1.02 to 7.67 ± 1.36 nmol PNP $g^{-1}h^{-1}$ (Fig. 3**h**). The range of soil ALP activity varied from 21.86 ± 2.81 to 50.74 ± 8.18 nmol PNP $g^{-1}h^{-1}$ (Fig. 3**i**). Soil fungal biomass, soil fungi/bacteria ratios, root AMF biomass, and soil ALP activity were consistent between salinity treatment groups during short-term salinization, whereas they all increased with increasing salinity during long-term salinization

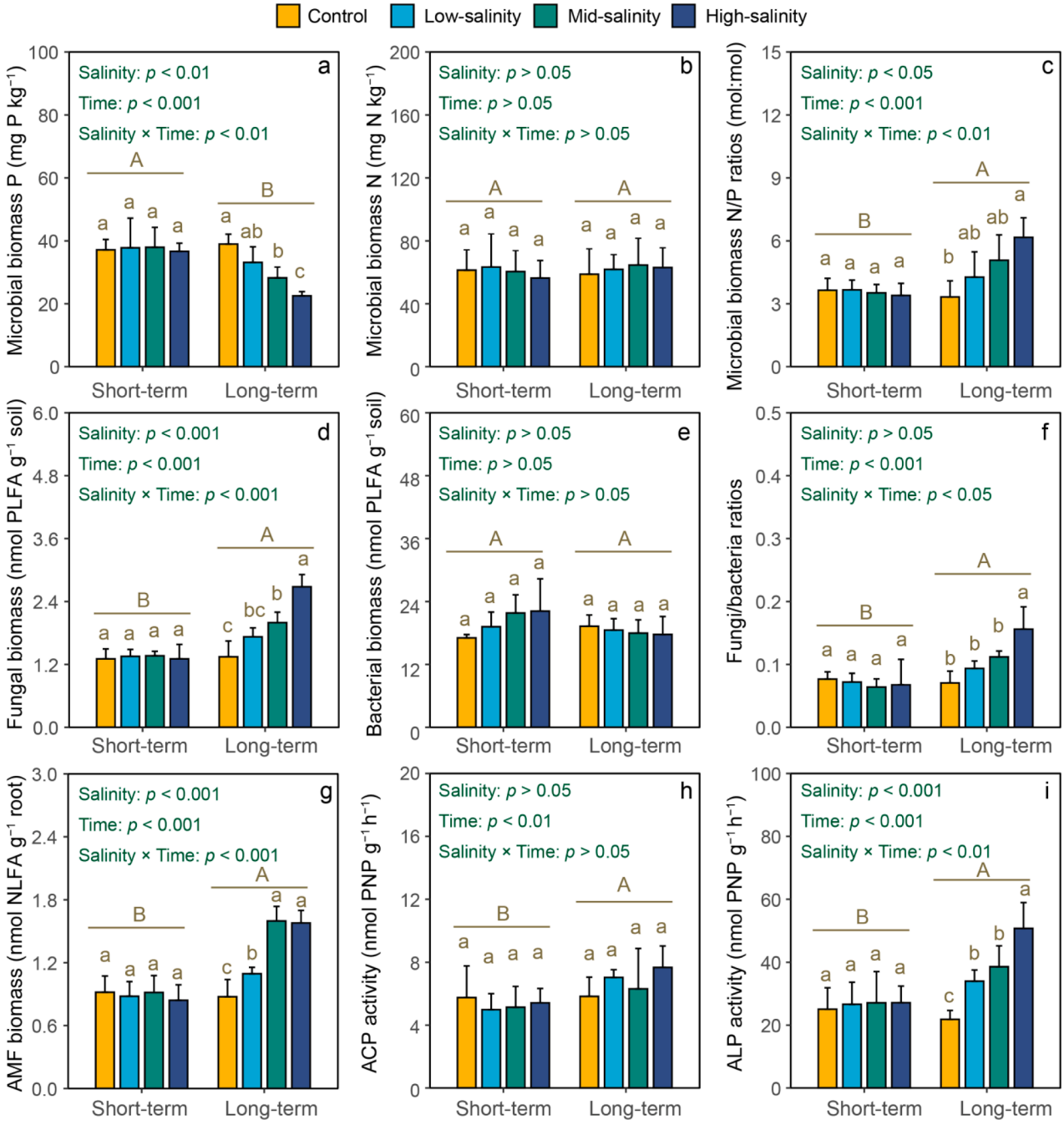


Fig. 3. Changes in microbial properties under short- and long-term salinization. Data are presented as the mean ± standard deviation (n = 5). Capital letters indicate significant differences ($p < 0.05$; *t*-test) between the short- and long-term experiment. Lowercase letters indicate significant differences ($p < 0.05$; Tukey's post hoc test) among the four salinity treatments within either the short- or long-term experiment. ACP: acid phosphomonoesterase; ALP: alkaline phosphomonoesterase; AMF: arbuscular mycorrhizal fungi; PLFA: phospholipid fatty acids; NLFA: neutral lipid fatty acids; PNP: p-nitrophenyl phosphate.

(Fig. 3**d, 3f, 3 g and 3i**). Soil bacterial biomass and ACP activity was consistent between salinity treatments for both short- and long-term salinization (Fig. 3**e and 3 h**).

3.3. Soil abiotic properties under salinization

The range of soil Fe(III) concentrations varied from 31.41 ± 4.02 to 56.07 ± 7.83 μmol Fe g^{-1}, while the range of soil Fe(II) concentrations varied from 13.16 ± 0.81 to 26.49 ± 2.61 μmol Fe g^{-1} (Table 1). The range of soil Fe sulfide concentrations varied from 0.49 ± 0.26 to 28.03 ± 1.20 μmol Fe g^{-1} (Table 1). During both long- and short-term salinization, soil Fe(III) and Fe(II) concentrations decreased with increasing salinity, whereas Fe sulfide concentrations increased (Table 1).

3.4. Soil phosphorus fractions under salinization

Available P concentrations (10.61–25.85 mg P kg^{-1}) accounted for only 2.25% to 4.50% of total P during short-term salinization and 1.41% to 4.10% during long-term salinization (Table 2). Moderately labile Pi pools ranged from 185.62 ± 7.79 to 230.54 ± 28.03 mg P kg^{-1} (Table 2), with labile Po varying from 3.57 ± 1.06 to 7.97 ± 3.24 mg P kg^{-1} (Table 2) and moderately labile Po ranging from 32.58 ± 1.82 to 49.00 ± 3.79 mg P kg^{-1} (Table 2). The range of primary mineral P varied from 210.44 ± 17.35 to 239.48 ± 8.74 mg P kg^{-1}, while the range of occluded P concentrations varied from 110.26 ± 11.16 to 143.22 ± 8.40 mg P kg^{-1} (Table 2). The range of soil total P concentrations varied from 592.64 ± 23.25 to 660.08 ± 31.25 mg P kg^{-1} (Table 2). Available P and moderately labile Pi pools decreased with increasing salinity during both short-term and long-term salinization (Table 2). The labile Po, moderately labile Po, primary mineral P, and total P concentrations did not change with increasing salinity during short-term salinization but all decreased with increasing salinity during long-term salinization (Table 2). The occluded P concentrations did not change with increasing salinity during short-term salinization but increased with increasing salinity during long-term salinization (Table 2).

3.5. Regulation of soil phosphorus fractions under salinization

According to the RDA, the main regulatory factors of soil P fractions varied between long- and short-term salinization (Fig. 4**a to 4d**). Fe sulfide and Fe(III) were the dominant environmental variables driving the changes in soil P fractions during short-term salinization (Fig. 4**a and 4b**). In contrast, ALP activity, root AMF biomass, and Fe sulfide concentrations were the environmental variables that drove the changes in soil P fractions during long-term salinization (Fig. 4**c and 4d**). The explanatory contributions of abiotic and biotic properties were 46.4% and 6.3%, respectively, during short-term salinization (Fig. 4**b**), whereas the explanatory contributions of abiotic and biotic properties were 23.7% and 35.7%, respectively, during long-term salinization (Fig. 4**d**).

Linear regression showed that the moderately labile Pi pool was positively related to Fe(III) concentrations and negatively related to Fe sulfide concentrations during both short- and long-term salinization (Fig. 5**a and 5b**). Moreover, the hydrolyzable Po pools were negatively related to ALP activities during long-term salinization (Fig. 5**c**). The primary mineral P pool was negatively correlated with root AMF biomass during long-term salinization (Fig. 5**d**).

The SEM results (Fig. 6**a**) suggested that during short-term salinization, changes in salinity were positively related to abiotic factors (path coefficient = 0.91). The abiotic properties were negatively related to the moderately labile Pi pool (path coefficient = − 0.56), which was positively related to the available P pool (path coefficient = 0.46). Under long-term salinization, changes in salinity were positively correlated with abiotic (path coefficient = 0.83) and biotic (path coefficient = 0.88) factors; abiotic factors were negatively related to the moderately labile Pi pool (path coefficient = − 0.52), whereas biotic factors were negatively related to the sum of hydrolyzable Po and primary mineral P pools (path coefficient = − 0.69). Finally, the moderately labile Pi pool (path coefficient = 0.36) and the sum of the hydrolyzable Po and primary mineral P pools (path coefficient = 0.61) were positively related to available P (Fig. 6**b**). The biotic factors and the sum of hydrolyzable Po and primary mineral P pool had the larger standardized total effect to available P during long-term salinization than short-term salinization, whereas the abiotic factors and the moderately labile Pi pool had the

Table 2
Changes in soil phosphorus (P) fractions (mean ± standard deviation, n = 5) measured by a modified Hedley procedure (Hedley et al., 1982; Tiessen and Moir, 2007) after experimental salinization in tidal wetlands of the Min River Estuary, East China Sea.

Time	Treatment	Available P mg P kg^{-1}	Labile Po mg P kg^{-1}	Moderately labile Pi mg P kg^{-1}	Moderately labile Po mg P kg^{-1}	Primary mineral P mg P kg^{-1}	Occluded P mg P kg^{-1}	Total P mg P kg^{-1}
Short-term	**Control**	25.85 ± 2.70 Aa	7.37 ± 2.85 Aa	214.77 ± 16.10 Aa	42.52 ± 4.52 Aa	221.61 ± 27.11 Aa	114.26 ± 36.85 Aa	626.39 ± 48.39 Aa
	Low-salinity	21.94 ± 2.53 Aa	7.72 ± 2.32 Aa	215.65 ± 8.98 Aa	41.26 ± 9.27 Aa	211.85 ± 12.99 Aa	123.46 ± 7.37 Aa	621.88 ± 15.16 Aa
	Mid-salinity	23.38 ± 2.12 Aa	7.10 ± 2.28 Aa	208.97 ± 23.37 Aab	40.89 ± 14.95 Aa	225.52 ± 51.43 Aa	113.05 ± 23.34 Ba	618.91 ± 73.70 Aa
	High-salinity	16.12 ± 2.50 Ab	7.97 ± 3.24 Aa	185.62 ± 7.79 Ab	44.99 ± 12.42 Aa	216.27 ± 19.93 Aa	118.74 ± 12.67 Ba	589.71 ± 37.49 Aa
Long-term	**Control**	23.79 ± 2.92 Ba	7.02 ± 0.74 Ba	230.54 ± 28.03 Aa	49.00 ± 3.79 Aa	239.48 ± 8.74 Aa	110.26 ± 11.16 Ab	660.08 ± 31.25 Aa
	Low-salinity	19.05 ± 1.31 Bb	4.31 ± 1.67 Bb	213.82 ± 16.84 Aab	43.59 ± 2.77 Aab	232.41 ± 16.13 Aab	127.90 ± 8.16 Aa	641.08 ± 12.85 Aab
	Mid-salinity	15.96 ± 3.31 Bb	4.34 ± 1.46 Bb	206.65 ± 15.72 Aab	38.06 ± 4.19 Abc	223.10 ± 16.49 Aab	136.80 ± 10.01 Aa	624.91 ± 10.81 Aab
	High-salinity	10.61 ± 2.02 Bc	3.57 ± 1.06 Bb	192.22 ± 15.21 Ab	32.58 ± 1.82 Ac	210.44 ± 17.35 Ab	143.22 ± 8.40 Aa	592.64 ± 23.25 Ab
Source of variation [a]								
Salinity		**	*n.s.*	**	*n.s.*	*n.s.*	*n.s.*	*
Time		***	***	*n.s.*	*n.s.*	*n.s.*	*	*n.s.*
Salinity × Time		***	*n.s.*	*n.s.*	*n.s.*	*n.s.*	*n.s.*	*n.s.*

Capital letters indicate significant differences ($p < 0.05$; *t*-test) between the short- and long-term experiments. Lowercase letters indicate significant differences ($p < 0.05$; Tukey's post hoc test) among the four salinity treatments within either the short- or long-term experiment.
(*n.s.*, not significant; *$p < 0.05$, **$p < 0.01$, and ***$p < 0.001$).
Pi: inorganic P; Po: organic P.
[a] The experiment times are as follows: short-term = 6 months and long-term = 3.5 years.

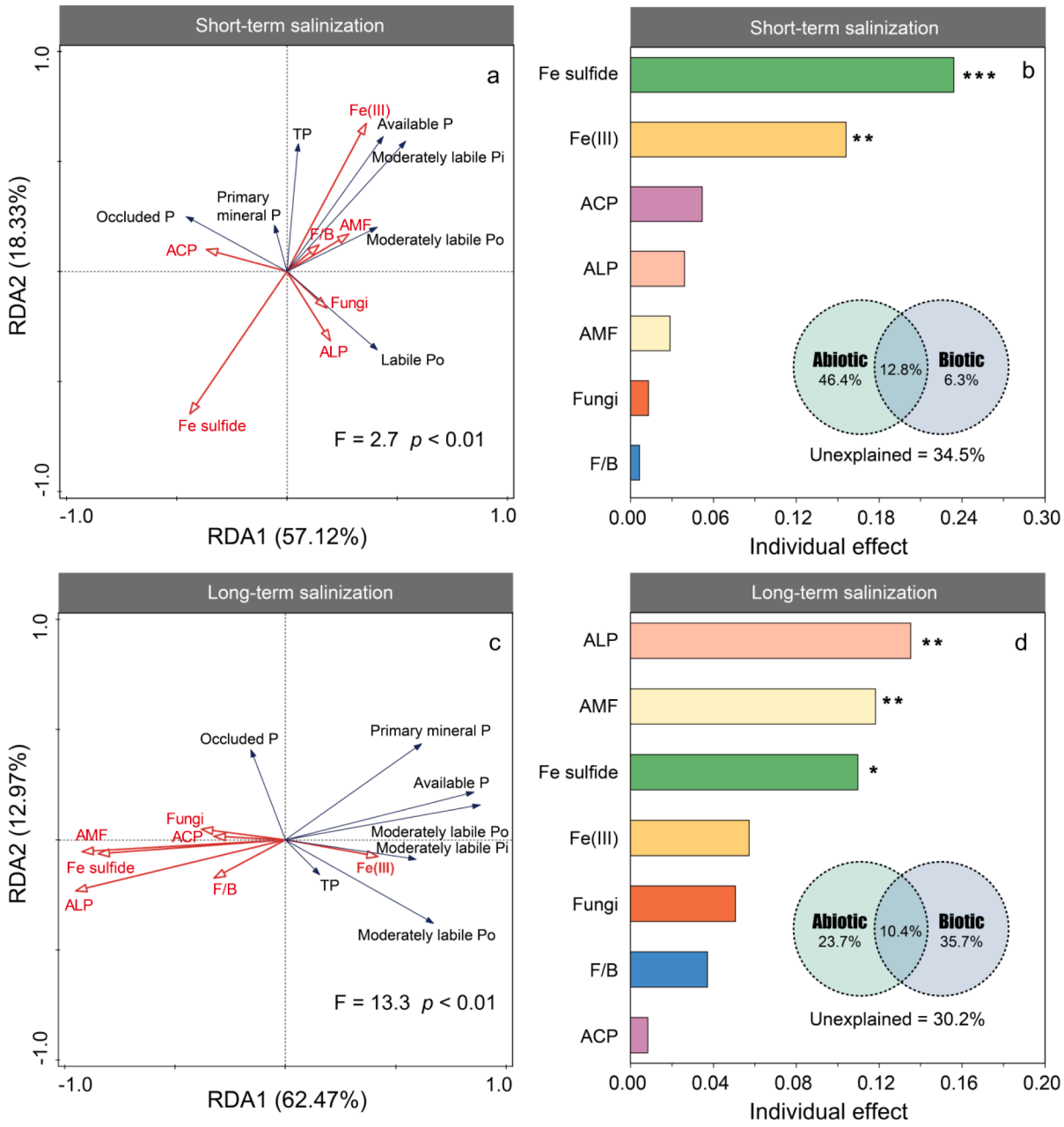


Fig. 4. Redundancy analysis (RDA) to determine the relationship between soil phosphorus (P) fractions and environmental factors under short- (a) and long-term (c) salinization. The right two panels present the individual effect of each environmental factor on the changes in soil P fractions under short- (b) and long-term (d) salinization. In (b) and (d), * indicates a significant effect of environmental factors on the changes in soil P fractions (*$p < 0.05$, **$p < 0.01$, and ***$p < 0.001$). The middle panels depicted in (b) and (d) show the results of variance partitioning analysis, which aimed to explain the relative contributions of biotic and abiotic factors to the response to short- and long-term salinization. ACP: acid phosphomonoesterase; ALP: alkaline phosphomonoesterase; AMF: arbuscular mycorrhizal fungi; F/B: the ratio of fungi to bacteria.

relatively greater standardized total effect to available P during short-term salinization than long-term salinization (Fig. 6**c**).

4. Discussion

4.1. Long-term salinization exacerbates ecosystem phosphorus limitation

Our results showed that ecosystem P limitation was exacerbated as salinization extended from short- to long-term in the experimental mesocosms (supporting Hypothesis I). We present two lines of evidence for this. First, changes in plant N/P ratios indicated ecosystem P limitation. Generally, a plant N/P ratio greater than 16 indicates an ecosystem P limitation, whereas a plant N/P ratio < 14 indicates an ecosystem N limitation in tidal wetlands (Więski et al., 2010; Hu et al., 2022a). In the current study, plant N/P ratios exceeded 16 during short- and long-term salinization (Fig. 2**c**), indicating that ecosystem P limitation rather than N limitation was prevailing under salinization in the tidal wetland. Moreover, plant N/P ratios did not change during short-term salinization but increased with salinization during long-term salinization (Fig. 2**c**), indicating that short-term salinization did not alter ecosystem P limitation but that long-term salinization exacerbated it. Second, the changes in microbial biomass N/P ratios also reflected ecosystem P limitation. When the availability of soil P is limited, competition for P between plants and microbes increased, and soil microbes generally showed reduced accumulation of P for their cells, resulting in an increase in microbial biomass N/P ratios (Cui et al.,

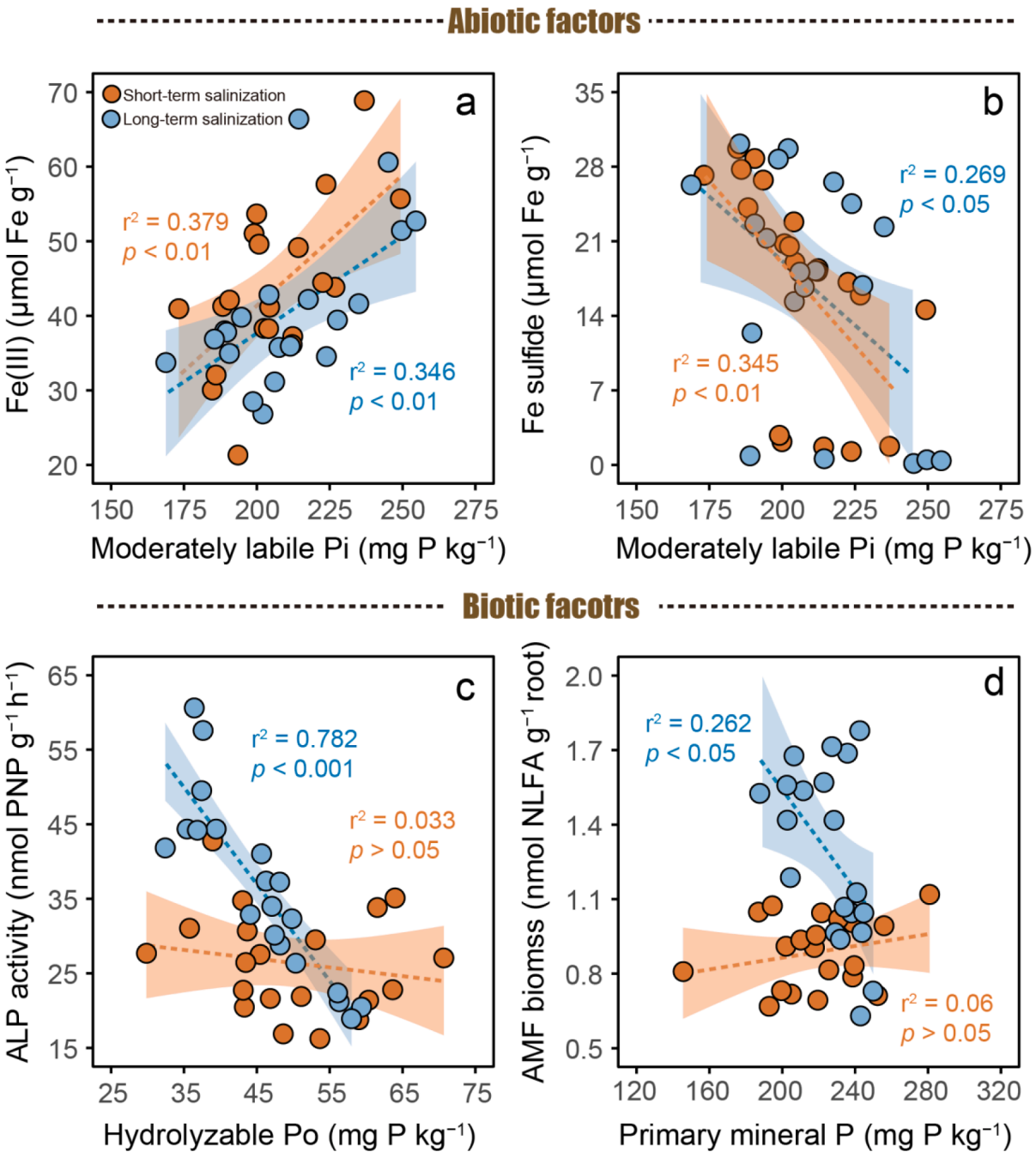


Fig. 5. Relationships between soil phosphorus (P) fractions and abiotic and biotic factors under short- and long-term salinization. Hydrolyzable Po: the sum of moderately labile Po and labile Po; ALP: alkaline phosphomonoesterase; AMF: arbuscular mycorrhizal fungi; Pi: inorganic P; Po: organic P.

2021). Therefore, the microbial biomass N/P ratios did not change with increasing salinity during short-term salinization but decreased as salinity increased during long-term salinization (Fig. 3**c**), implying that soil P availability limits the microbial P demand during long-term salinization.

The exacerbated ecosystem P limitation during long-term salinization could be attributed to a decrease in soil P availability. There are three possible explanations for this. First, the soil-occluded P pool increased, whereas the labile P pool decreased, under long-term salinization (Table 2), suggesting that parts of the labile P were transformed to recalcitrant P when salinization was extended from the short to long term. This occurs because plants and microbes can incorporate labile P into their cells and yield structurally complex macromolecule organic P that are less available (Liu et al., 2021; Hu et al., 2022a). Second, total plant biomass did not decrease with increasing salinity during long-term salinization (Fig. 2**f**). To maintain high plant productivity under salt stress, plants would adsorb a large amount of P from soils, which exacerbated ecosystem P limitation during long-term salinization (Li et al., 2016; Chen et al., 2020; Luo et al., 2022). Third, salinization could increase P desorption, and a part of the dissolved P might be taken away by the tidewaters during long-term salinization (Noe et al., 2012; Bai et al., 2017; Nguyen et al., 2019). Nevertheless, our results suggested that ecosystem P limitation was exacerbated as salinization extended from short- to long-term, leading to the next question of how tidal wetland ecosystems acquire P under more P-limited condition.

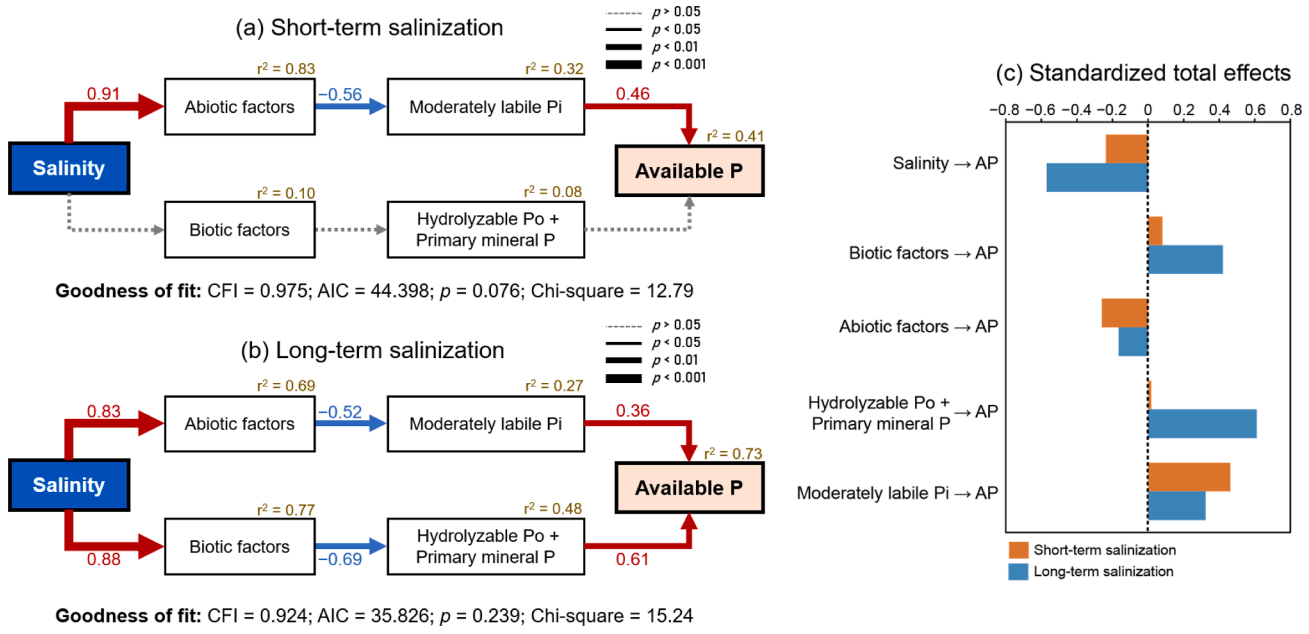


Fig. 6. Structural equation model (SEM) outcomes of expected causal relationships under short-term (a) and long-term (b) salinization, as well as the standardized total effects on available phosphorus (c). Red and blue arrows represent positive and negative relationships, respectively. Numbers on arrows represent standardized path coefficients, and arrow widths represent the significance level. Values above the rectangles represent the explained variance (r^2) of the variables. Abiotic factors included Fe sulfide concentrations, whereas biotic factors included alkaline phosphomonoesterase (ALP) activities and arbuscular mycorrhizal fungi (AMF) biomass; Pi: inorganic P; Po: organic P; AP: available P. (For interpretation of the references to colour in this figure legend, the reader is referred to the web version of this article.)

4.2. Role of abiotic phosphorus-acquisition strategy under salinization

The mobilization of soil moderately labile Pi could be a source of available P during both short- and long-term salinization (supporting Hypothesis II). This was directly supported by the decrease in the moderately labile Pi pool as salinity increased during both short- and long-term salinization (Table 2). Furthermore, the mobilization of moderately labile Pi was accompanied by Fe(III) reduction and Fe sulfide accumulation (Fig. 5**a and 5b**). This occurs because moderately labile Pi in tidal wetland soils mainly consists of Fe(III)-bound P (Xu et al., 2012; Hu et al., 2020). Under salinization, sulfate reduction promotes sulfide accumulation (Burton et al., 2006; Luo et al., 2019). When sulfide (a strong reductant) is present, Fe(III)-bound P precipitates with sulfides as Fe sulfides (Lehtoranta et al., 2009; Luo et al., 2015) and releases P from Fe(III)-bound P (Jordan et al., 2008; Jun et al., 2013; Bai et al., 2017). Therefore, our results suggest that both short- and long-term salinization mobilize moderately labile Pi and increase P availability through abiotic processes. This abiotic P-acquisition strategy might satisfy plant and microbial P demand during short-term salinization since ecosystem P limitation was not altered during short-term salinization. However, as ecosystem P limitation was exacerbated during long-term salinization, alternative P-acquisition strategies could exist.

4.3. Role of biotic phosphorus-acquisition strategy under salinization

Our results showed that the hydrolyzable Po (the sum of moderately labile Po and labile Po) pool decreased during long-term salinization (Table 2). Additionally, soil ALP activities—proxies of Po mineralization—were negatively correlated with the hydrolyzable Po pool during long-term salinization (Fig. 5**c**). These results indicate that hydrolyzable Po was mineralized via the production of ALP during long-term salinization. Furthermore, the ALP activities were positively correlated with fungal biomass and fungi/bacteria ratios under long-term salinization (Fig. S3**a and S3b**). In contrast to the unchanged microbial PLFAs during short-term salinization, long-term salinization increased the fungal biomass but did not affect the bacterial biomass, leading to higher fungi/bacteria ratios (Fig. 3**d to 3f**). These results indicate that soil microbes might shift their community composition to increase phosphatase production under salinization. This occurs because, compared to bacteria (copiotrophs), most fungi (oligotrophs) are more tolerant to low-nutrient environments (Rath and Rousk, 2015; Li et al., 2016) and have a greater capacity to produce extracellular enzymes to cleave Po (Hu et al., 2022a). For example, our previous studies suggested that salinization results in significant accumulation of the fungal phyla Claroideoglomus and Funneliformis in the tidal wetland soils (Chen et al., 2022a; Chen et al., 2022b), which both have the capacity for the production of phosphatase (Carballar-Hernández et al., 2017; Sang et al., 2022). In addition, some tidal wetland plants also could produce phosphatases during P limitation. For example, some Cyperaceae members could form dauciform roots and release phosphatases under P deficiency (Güsewell et al., 2007). Overall, the enhancement of ALP production could be considered a biotic P-acquisition strategy in tidal wetlands under long-term salinization.

The primary mineral P pool decreased during long-term salinization (Table 2), suggesting that primary mineral P could also be a source of available P during long-term salinization. Additionally, the primary mineral P pool was negatively correlated with root AMF biomass during long-term salinization (Fig. 5**d**). These results demonstrate that *C. malaccensis* formed a symbiotic relationship with AMF and that changes in the soil primary mineral P were related to the variations in AMF symbiosis under salinization. Plants in waterlogged environments usually are considered to lack AMF associations (Tester et al., 1987; Muthukumar et al., 2003). However, increasing studies have found the AMF colonization is present in the root samples of various wetland sedges (Zhang et al., 2014; Xu et al., 2016; Ramírez-Viga et al., 2018), even including some species that are considered to be members of predominantly non-mycorrhizal families, such as Cyperaceae (Brundrett, 2002; Muthukumar et al., 2004). Indeed, a previous study showed the arbuscular colonization (10–30%) of *C. malaccensis* in the southwest coast of India (Sridhar et al., 2011). Sengupta and Chaudhuri (2002) also identified hyphae, glomus-type vesicles, and arbuscules in the roots of

C. malaccensis. To further confirm that root of *C. malaccensis* could produce AMF to acquire P, we also examined the plant Mn concentrations (**Fig. S2**), a proxy for rhizosphere carboxylate concentrations (Lambers et al., 2015; Liu et al., 2021). We found a strong positive correlation between root AMF biomass and plant Mn concentrations during long-term salinization (Fig. S3**c**), which implied that *C. malaccensis* enhanced AMF associations by stimulating carboxylate release to solubilize P. Therefore, our results suggested that the enhancement of root AMF association could also be a possible biotic P-acquisition strategy under long-term salinization.

Overall, our results provide support for Hypothesis III, demonstrating that the biotic P-acquisition strategies, such as soil ALP production and root AMF association, drove soil P transformation under long-term salinization conditions in tidal wetland soils.

4.4. Implication for future sea-level rise

Our results suggest that saltwater intrusion into freshwater wetlands might initially act as a P subsidy by stimulating abiotic P-acquisition strategies. However, chronic exposure to saltwater resulted in exaggerated P limitation. To maintain high primary productivity, tidal wetland plants and soil microbes adopted biotic P-acquisition strategies to acquire P under conditions of prolonged salinization (Fig. 7). These biotic P-acquisition strategies have been overlooked for a long time, as the majority of previous studies concerning soil P transformation in tidal wetlands were conducted in a laboratory without plants or were based on short-term field experiments (Jordan et al., 2008; Chambers et al., 2013). However, the relatively long-term (3.5 years) mesocosm experiment applied in our study allowed for the development of biotic P-acquisition strategies under increased salinity. These biotic P-acquisition strategies could be considered the acclimation of tidal wetland ecosystems to more-P limited conditions under increasing salt stress (Yang et al., 2022; Zhai et al., 2022). Owing to biotic P-acquisition strategies, ecosystem P limitation was alleviated to a certain degree. Thus, tidal wetland ecosystems could maintain high plant primary productivity under long-term salinization. Consequently, the tidal wetland ecosystems might have a better chance to keep pace with the sea level rise.

4.5. Limitations for this study

The present study has some limitations. First, plant Mn concentrations were adopted as a proxy for carboxylate concentrations in the soils. Future studies could instead consider applying both ^{13}C and ^{14}C isotope-labeled carboxylates to assess their role in mobilizing primary mineral P in tidal wetlands. Second, only one salt-tolerant tidal wetland plant species was investigated in this study. The selected tidal wetland plant *C. malaccensis* could show root AMF associations to acquire P. Future studies should include plants with and without root AMF associations to compare their P-acquisition strategies under salinization. Third, changes in the hydrologic context were accompanied by salinization under conditions of a rising sea level. A previous study showed that increasing flooding alters the response of Fe-bound P to salinization (Bai et al., 2017). Thus, comparative laboratory and field studies are required to ascertain the synergistic effects of tidal inundation and salinization on soil P transformation. Last, sequential P fractionation, especially the Hedley method, is widely used for soil P transformation. However, all P fractionations are operationally defined and might lack chemical precision (Kar et al., 2011; Klotzbücher et al., 2019). Advanced techniques, such as P k-edge XANES (x-ray adsorption near edge structure), should be adopted in a future study. Regardless of these uncertainties, our study provides direct evidence demonstrating biotic P-acquisition strategies under long-term salinization, which has significant implications for ecosystem feedback in tidal wetlands under conditions of a rising sea level.

5. Conclusion

A mesocosm experiment was conducted to clarify how tidal wetland plants and soil microbes adapt to salinization-induced ecosystem P limitation over time in tidal wetland ecosystems. We found that short-term salinization induced abiotic processes [Fe(III) reduction and Fe sulfide accumulation], which stimulated the transformation from the moderately labile inorganic P pool to available P. Owing to this abiotic P-acquisition strategy, ecosystem P limitation was not altered by increasing salinity during short-term salinization. However, ecosystem P limitation was exacerbated with increasing salinity during long-term

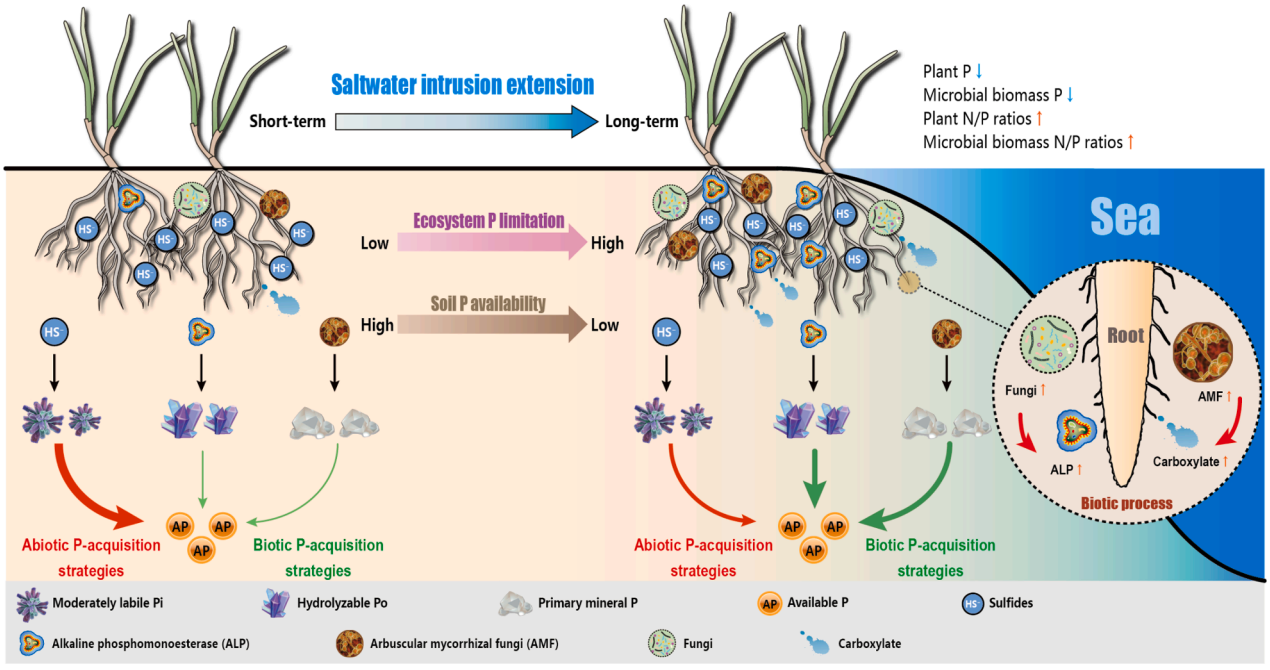


Fig. 7. Potential mechanisms for abiotic and biotic phosphorus-acquisition strategies during short- and long-term salinization in the tidal freshwater wetland ecosystem. Arrow widths represent the contribution of each phosphorus-acquisition strategy.

salinization. In addition to abiotic P-acquisition, we also observed that tidal wetland ecosystems adopted biotic P-acquisition (including ALP production and AMF association) to mobilize hydrolyzable Po and primary mineral P. The transformation of hydrolyzable Po and primary mineral P to available P could alleviate the increased ecosystem P limitation during long-term salinization to some extent, maintaining the high primary productivity of tidal wetland ecosystems. This study furthers our comprehension of the underlying mechanisms that determine the tidal wetland ecosystem functional responses to the impending salinization caused by sea-level rise. We recommend that future earth system models should include biotic P-acquisition strategies when predicting the responses of soil P transformation in tidal wetlands to future sea-level rise.

Supplementary material.

Supplementary material is available for three figures.

CRediT authorship contribution statement

Tianning Fan: Formal analysis, Investigation, Writing – original draft. **Min Luo:** Conceptualization, Methodology, Writing – original draft, Supervision, Project administration. **Ji Tan:** Formal analysis, Investigation, Writing – original draft. **Dehong Hu:** Formal analysis, Investigation. **Xin Chen:** Investigation, Formal analysis. **Jiafang Huang:** Investigation, Formal analysis, Project administration. **Shihua Li:** Investigation, Formal analysis. **Pingping Guo:** Investigation, Formal analysis. **Ji Chen:** Conceptualization, Methodology, Supervision.

Declaration of Competing Interest

The authors declare that they have no known competing financial interests or personal relationships that could have appeared to influence the work reported in this paper.

Data availability

Data have been deposited in figshare, https://figshare.com/s/ced0bed3aa31f7748ecb

Acknowledgements

This work was financially supported by grants from the National Science Foundation of China (No. 32071598; 41501252), the Natural Science Foundation of Fujian Province (No. 2020J01503), the Science and Technology Projects of the Forest Bureau of Fujian Province (No. 2021FKJ30), and the Public Welfare Project of Science and Technology Department of Fujian Province (No. 2022R1002007).

Appendix A. Supplementary data

Supplementary data to this article can be found online at https://doi.org/10.1016/j.catena.2023.107274.

References

Abell, G.C., Ross, D.J., Keane, J.P., Oakes, J.M., Eyre, B.D., Robert, S.S., Volkman, J.K., 2013. Nitrifying and denitrifying microbial communities and their relationship to nutrient fluxes and sediment geochemistry in the Derwent Estuary. Tasmania. Aquat. Microb. Ecol. 70, 63–75. https://doi.org/10.3354/ame01642.

Bai, J., Ye, X., Jia, J., Zhang, G., Zhao, Q., Cui, B., Liu, X., 2017. Phosphorus sorption-desorption and effects of temperature, pH and salinity on phosphorus sorption in marsh soils from coastal wetlands with different flooding conditions. Chemosphere 188, 677–688. https://doi.org/10.1016/j.chemosphere.2017.08.117.

Brookes, P.C., Powlson, D.S., Jenkinson, D.S., 1982. Measurement of microbial biomass phosphorus in soil. Soil Biol. Biochem. 14, 319–329. https://doi.org/10.1016/0038-0717(82)90001-3.

Brundrett, M.C., 2002. Coevolution of roots and mycorrhizas of land plants. New Phytol. 154, 275–304. https://doi.org/10.1046/j.1469-8137.2002.00397.x.

Burton, E.D., Bush, R.T., Sullivan, L.A., 2006. Acid-volatile sulfide oxidation in coastal flood plain drains: iron-sulfur cycling and effects on water quality. Environ. Sci. Technol. 40, 1217–1222. https://doi.org/10.1021/es0520058.

Carballar-Hernández, S., Hernández-Cuevas, L.V., Montaño, N.M., Larsen, J., Ferrera-Cerrato, R., Taboada-Gaytán, O.R., Montiel-González, A.M., Alarcón, A., 2017. Native communities of arbuscular mycorrhizal fungi associated with *Capsicum annuum* L. respond to soil properties and agronomic management under field conditions. Agric. Ecosyst. Environ. 245, 43–51. https://doi.org/10.1016/j.agee.2017.05.004.

Carvalho, L.M., Correia, P.M., Caçador, I., Martins-Loução, M.A., 2003. Effects of salinity and flooding on the infectivity of salt marsh arbuscular mycorrhizal fungi in *Aster tripolium* L. Biol. Fertil. Soils 38, 137–143. https://doi.org/10.1007/s00374-003-0621-6.

Chambers, L.G., Osborne, T.Z., Reddy, K.R., 2013. Effect of salinity-altering pulsing events on soil organic carbon loss along an intertidal wetland gradient: a laboratory experiment. Biogeochemistry 115, 363–383. https://doi.org/10.1007/s10533-013-9841-5.

Chen, J., Groenigen, K.J., Hungate, B.A., Terrer, C., Groenigen, J., Maestre, F.T., Ying, S. C., Luo, Y., Jørgensen, U., Sinsabaugh, R.L., Olesen, J.E., Elsgaard, L., 2020. Long-term nitrogen loading alleviates phosphorus limitation in terrestrial ecosystems. Glob. Change Biol. 26, 5077–5086. https://doi.org/10.1111/gcb.15218.

Chen, X., Jiang, N., Condron, L.M., Dunfield, K.E., Chen, Z., Wang, J., Chen, L., 2019. Soil alkaline phosphatase activity and bacterial phoD gene abundance and diversity under long-term nitrogen and manure inputs. Geoderma 349, 36–44. https://doi.org/10.1016/j.geoderma.2019.04.039.

Chen, X., Luo, M., Liu, Y., Tan, J., Zhang, C., Tan, F., Huang, J., 2022a. Linking carbon-degrading enzyme activity to microbial carbon-use trophic strategy under salinization in a subtropical tidal wetland. Appl. Soil Ecol. 174, 104421 https://doi.org/10.1016/j.apsoil.2022.104421.

Chen, X., Luo, M., Tan, J., Zhang, C., Liu, Y., Huang, J., Tan, Y., Xiao, L., Xu, Z., 2022b. Salt-tolerant plant moderates the effect of salinity on soil organic carbon mineralization in a subtropical tidal wetland. Sci. Total Environ. 837, 155855 https://doi.org/10.1016/j.scitotenv.2022.155855.

Craft, C., 2007. Freshwater input structures soil properties, vertical accretion, and nutrient accumulation of Georgia and U.S. tidal marshes. Limnol. Oceanogr. 52, 1220–1230. https://doi.org/10.4319/lo.2007.52.3.1220.

Cui, Y., Bing, H., Fang, L., Jiang, M., Shen, G., Yu, J., Wang, X., Zhu, H., Wu, Y., Zhang, X., 2021. Extracellular enzyme stoichiometry reveals the carbon and phosphorus limitations of microbial metabolisms in the rhizosphere and bulk soils in alpine ecosystems. Plant Soil 458, 7–20. https://doi.org/10.1007/s11104-019-04159-x.

Dang, C., Morrissey, E.M., Neubauer, S.C., Franklin, R.B., 2019. Novel microbial community composition and carbon biogeochemistry emerge over time following saltwater intrusion in wetlands. Glob. Chang Biol. 25, 549–561. https://doi.org/10.1111/gcb.14486.

Ding, W., Cong, W.F., Lambers, H., 2021. Plant phosphorus-acquisition and-use strategies affect soil carbon cycling. Trends Ecol. Evol. 36, 899–906. https://doi.org/10.1016/j.tree.2021.06.005.

Drake, D.R., Ungar, I.A., 1989. Effects of salinity, nitrogen, and population density on the survival, growth, and reproduction of *Atriplex triangularis* (Chenopodiaceae). Am. J. Bot. 76, 1125–1135. https://doi.org/10.1002/j.1537-2197.1989.tb15097.x.

Flower, H., Rains, M., Lewis, D., Zhang, J., 2017. Rapid and intense phosphate desorption kinetics when saltwater intrudes into carbonate rock. Estuar. Coasts 40, 1301–1313. https://doi.org/10.1007/s12237-017-0228-z.

Frostegård, A., Bååth, E., 1996. The use of phospholipid fatty acid analysis to estimate bacterial and fungal biomass in soil. Biol. Fertil. Soils 22, 59–65. https://doi.org/10.1007/BF00384433.

Gupta, N., Bihari, K.M., Sengupta, I., 2016. Diversity of arbuscular mycorrhizal fungi in different salinity of mangrove ecosystem of Odisha, India. Adv. Plants Agric. Res. 3, 19–23. https://doi.org/10.15406/apar.2016.03.00085.

Güsewell, S., Pohl, M., Gander, A., Strehler, C., 2007. Temporal changes in grazing intensity and herbage quality within a Swiss fen meadow. Alp. Botany 117, 57–73. https://doi.org/10.1007/s00035-007-0798-7.

Hartzell, J.L., Jordan, T.E., Cornwell, J.C., 2017. Phosphorus sequestration in sediments along the salinity gradients of Chesapeake Bay subestuaries. Estuar. Coasts 40, 1607–1625. https://doi.org/10.1007/s12237-017-0233-2.

Hedley, M.J., Stewart, J.W.B., Chauhan, B., 1982. Changes in inorganic and organic soil phosphorus fractions induced by cultivation practices and by laboratory incubations. Soil Sci. Soc. Am. J. 46, 970–976. https://doi.org/10.2136/sssaj1982.03615995004600050017x.

Herbert, E.R., Boon, P., Burgin, A.J., Neubauer, S.C., Franklin, R.B., Ardón, M., Hopfensperger, K.N., Lamers, L.P.M., Gell, P., 2015. A global perspective on wetland salinization: Ecological consequences of a growing threat to freshwater wetlands. Ecosphere 6, 1–43. https://doi.org/10.1890/ES14-00534.1.

Hou, E., Luo, Y., Kuang, Y., Chen, C., Lu, X., Jiang, L., Luo, X., Wen, D., 2020. Global meta-analysis shows pervasive phosphorus limitation of aboveground plant production in natural terrestrial ecosystems. Nat. Commun. 11, 637. https://doi.org/10.1038/s41467-020-14492-w.

Hu, Y., Chen, J., Hui, D., Wang, Y.P., Li, J., Chen, J., Chen, G., Zhu, Y., Zhang, L., Zhang, D., Deng, Q., 2022a. Mycorrhizal fungi alleviate acidification-induced phosphorus limitation: Evidence from a decade-long field experiment of simulated acid deposition in a tropical forest in south China. Glob. Change Biol. 18, 3605–3619. https://doi.org/10.1111/gcb.16135.

Hu, M., Peñuelas, J., Sardans, J., Tong, C., Chang, C., Cao, W., 2020. Dynamics of phosphorus speciation and the phoD phosphatase gene community in the

rhizosphere and bulk soil along an estuarine freshwater-oligohaline gradient. Geoderma 365, 114236. https://doi.org/10.1016/j.geoderma.2020.114236.
Hu, M., Sardans, J., Le, Y., Yan, R., Zhong, Y., Huang, J., Peñuelas, J., Tong, C., 2022b. Biogeochemical behavior of P in the soil and porewater of a low-salinity estuarine wetland: Availability, diffusion kinetics, and mobilization mechanism. Water Res. 219, 118617 https://doi.org/10.1016/j.watres.2022.118617.
Hyun, J.H., Smith, A.C., Kostka, J.E., 2007. Relative contributions of sulfate-and iron(III) reduction to organic matter mineralization and process controls in contrasting habitats of the Georgia saltmarsh. Appl. Geochem. 22, 2637–2651. https://doi.org/10.1016/j.apgeochem.2007.06.005.
Ipcc, 2022. In: Climate change 2022: impacts, adaptation, and vulnerability. Contribution of working Group II to the sixth assessment report of the intergovernmental panel on climate change. Cambridge University Press, pp. 3–33. https://doi.org/10.1017/9781009325844.001.
Jarosch, K.A., Kandeler, E., Frossard, E., Bünemann, E.K., 2019. Is the enzymatic hydrolysis of soil organic phosphorus compounds limited by enzyme or substrate availability? Soil Biol. Biochem. 139, 107628 https://doi.org/10.1016/j.soilbio.2019.107628.
Jordan, T.E., Cornwell, J.C., Boynton, W.R., Anderson, J.T., 2008. Changes in phosphorus biogeochemistry along an estuarine salinity gradient: The iron conveyer belt. Limnol. Oceanogr. 53, 172–184. https://doi.org/10.4319/lo.2008.53.1.0172.
Jun, M., Altor, A.E., Craft, C.B., 2013. Effects of increased salinity and inundation on inorganic nitrogen exchange and phosphorus sorption by tidal freshwater floodplain forest soils, Georgia (USA). Estuar. Coasts 36, 508–518. https://doi.org/10.1007/s12237-012-9499-6.
Kar, G., Hundal, L.S., Schoenau, J.J., Peak, D., 2011. Direct chemical speciation of P in sequential chemical extraction residues using P K-Edge X-Ray Absorption Near-Edge Structure Spectroscopy. Soil Sci. 176, 589–595. https://doi.org/10.1097/SS.0b013e31823939a3.
Keene, A.F., Johnston, S.G., Bush, R.T., Sullivan, L.A., Burton, E.D., McElnea, A.E., Ahern, C.R., Powell, B., 2011. Effects of hyper-enriched reactive Fe on sulfidisation in a tidally inundated acid sulfate soil wetland. Biogeochemistry 103, 263–279. https://doi.org/10.1007/s10533-010-9461-2.
Klotzbücher, A., Kaiser, K., Klotzbücher, T., Wolff, M., Mikutta, R., 2019. Testing mechanisms underlying the Hedley sequential phosphorus extraction of soils. J. Plant Nutr. Soil Sci. 182, 570–577. https://doi.org/10.1002/jpln.201800652.
Kostka, J.E., Dalton, D.D., Skelton, H., Dollhopf, S., Stucki, J.W., 2002. Growth of Iron (III)-reducing bacteria on clay minerals as the sole electron acceptor and comparison of growth yields on a variety of oxidized iron forms. Appl. Environ. Microb. 68, 6256–6262. https://doi.org/10.1128/AEM.68.12.6256-6262.2002.
Kristensen, E., Mangion, P., Tang, M., Flindt, M.R., Holmer, M., Ulomi, S., 2011. Microbial carbon oxidation rates and pathways in sediments of two Tanzanian mangrove forests. Biogeochemistry 103, 143–158. https://doi.org/10.1007/s10533-010-9453-2.
Lambers, H., Cawthray, G.R., Giavalisco, P., Kuo, J., Laliberté, E., Pearse, S.J., Scheible, W., Stitt, M., Teste, F., Turner, B.L., 2012. Proteaceae from severely phosphorus-impoverished soils extensively replace phospholipids with galactolipids and sulfolipids during leaf development to achieve a high photosynthetic phosphorus-use-efficiency. New Phytol. 196, 1098–1108. https://doi.org/10.1111/j.1469-8137.2012.04285.x.
Lambers, H., Hayes, P.E., Laliberte, E., Oliveira, R.S., Turner, B.L., 2015. Leaf manganese accumulation and phosphorus-acquisition efficiency. Trends Plant Sci. 20, 83–90. https://doi.org/10.1016/j.tplants.2014.10.007.
Lamers, L.P.M., Govers, L.L., Janssen, I.C.J.M., Geurts, J.J.M., Van Der Welle, M.E.W., Van Katwijk, M.M., Van Der Heide, T., Roelofs, J.G.M., Smolders, A.J.P., 2013. Sulfide as a soil phytotoxin—a review. Front. Plant Sci. 4 https://doi.org/10.3389/fpls.2013.00268.
Lehtoranta, J., Ekholm, P., Pitkänen, H., 2009. Coastal eutrophication thresholds: a matter of sediment microbial processes. Ambio 38, 303–308. https://doi.org/10.1579/09-A-656.1.
Li, Y., Niu, S., Yu, G., 2016. Aggravated phosphorus limitation on biomass production under increasing nitrogen loading: a meta-analysis. Glob. Change Biol. 22, 934–943. https://doi.org/10.1111/gcb.13125.
Liu, Y., Luo, M., Chen, J., Ye, R., Tan, J., Zhai, Z., Yang, Y., Huang, J., 2021. Root iron plaque abundance as an indicator of carbon decomposition rates in a tidal freshwater wetland in response to salinity and flooding. Soil Biol. Biochem. 162, 108403 https://doi.org/10.1016/j.soilbio.2021.108403.
Luo, M., Zeng, C., Tong, C., Huang, J., Yu, Q., Guo, Y., Wang, S., 2014. Abundance and speciation of iron across a subtropical tidal marsh of the Min River Estuary in the East China Sea. Appl. Geochem. 45, 1–13. https://doi.org/10.1016/j.apgeochem.2014.02.014.
Luo, M., Zeng, C., Tong, C., Huang, J., Yu, Q., Guo, Y., Wang, S., 2015. Kinetics of chemical and microbial iron reduction along an inundation gradient in a tidal marsh of the Min River Estuary, southeastern China. Geomicrobiol. J. 32, 635–647. https://doi.org/10.1080/01490451.2014.950362.
Luo, M., Huang, J., Zhu, W., Tong, C., 2019. Impacts of increasing salinity and inundation on rates and pathways of organic carbon mineralization in tidal wetlands: a review. Hydrobiologia 827, 31–49. https://doi.org/10.1007/s10750-017-3416-8.
Luo, M., Zhai, Z., Ye, R., Xing, R., Huang, J., Tong, C., 2020. Carbon mineralization in tidal freshwater marsh soils at the intersection of low-level saltwater intrusion and ferric iron loading. Catena 193, 104644. https://doi.org/10.1016/j.catena.2020.104644.
Luo, M., Moorhead, D.L., Ochoa-Hueso, R., Mueller, C.W., Ying, S.C., Chen, J., 2022. Nitrogen loading enhances phosphorus limitation in terrestrial ecosystems with implications for soil carbon cycling. Funct. Ecol. 36, 2845–2858. https://doi.org/10.1111/1365-2435.14178.
Marklein, A.R., Houlton, B.Z., 2012. Nitrogen inputs accelerate phosphorus cycling rates across a wide variety of terrestrial ecosystems. New Phytol. 193, 696–704. https://doi.org/10.1111/j.1469-8137.2011.03967.x.
Megonigal, J.P., Neubauer, S.C., 2009. Biogeochemistry of tidal freshwater wetlands. In: Coastal Wetlands: An Integrated Ecosystem Approach. Perillo, G.M.E., Wolanski, E., Cahoon, D.R., Brinson, M.M. (Eds.), Elsevier Cell Press, pp. 535–562. 10.1016/B978-0-444-63893-9.00019-8.
Morrissey, E.M., Gillespie, J.L., Morina, J.C., Franklin, R.B., 2014. Salinity affects microbial activity and soil organic matter content in tidal wetlands. Glob. Change Biol. 20, 1351–1362. https://doi.org/10.1111/gcb.12431.
Muthukumar, T., Sha, L., Yang, X., Cao, M., Tang, J., Zheng, Z., 2003. Mycorrhiza of plants in different vegetation types in tropical ecosystems of Xishuangbanna, southwest China. Mycorrhiza 13, 289–297. https://doi.org/10.1007/s00572-003-0234-9.
Muthukumar, T., Udaiyan, K., Shanmughavel, P., 2004. Mycorrhiza in sedges—an overview. Mycorrhiza 14, 65–77. https://doi.org/10.1007/s00572-004-0296-3.
Neubauer, S.C., 2013. Ecosystem responses of a tidal freshwater marsh experiencing saltwater intrusion and altered hydrology. Estuar. Coasts 36, 491–507. https://doi.org/10.1007/s12237-011-9455-x.
Neubauer, S.C., Craft, C.B., 2009. Global change and tidal freshwater wetlands: scenarios and impacts. In: Barendregt, A., Whigham, D.F., Baldwin, A.H. (Eds.), Tidal Freshwater Wetlands. Backhuys Publishers, pp. 253–266.
Neubauer, S.C., Franklin, R.B., Berrier, D.J., 2013. Saltwater intrusion into tidal freshwater marshes alters the biogeochemical processing of organic carbon. Biogeosciences 10, 8171–8183. https://doi.org/10.5194/bg-10-8171-2013.
Neumann, G., Martinoia, E., 2002. Cluster roots-an underground adaptation for survival in extreme environments. Trends Plant Sci. 7, 162–167. https://doi.org/10.1016/S1360-1385(02)02241-0.
Nguyen, T.T.N., Némery, J., Gratiot, N., Garnier, J., Strady, E., Tran, V.Q., Nguyen, A.T., Nguyen, T.N.T., Golliet, C., Aimé, J., 2019. Phosphorus adsorption/desorption processes in the tropical Saigon River estuary (Southern Vietnam) impacted by a megacity. Estuar. Coastal Shelf Sci. 227, 106321 https://doi.org/10.1016/j.ecss.2019.106321.
Noe, G.B., Krauss, K.W., Lockaby, B.G., Conner, W.H., Hupp, C.R., 2012. The effect of increasing salinity and forest mortality on soil nitrogen and phosphorus mineralization in tidal freshwater forested wetlands. Biogeochemistry 114, 225–244. https://doi.org/10.1007/s10533-012-9805-1.
Olsson, P.A., Bååth, E., Jakobsen, I., Söderström, B., 1995. The use of phospholipid and neutral lipid fatty acids to estimate biomass of arbuscular mycorrhizal fungi in soil. Mycol. Res. 99, 623–629. https://doi.org/10.1016/S0953-7562(09)80723-5.
Paludan, C., Morris, J.T., 1999. Distribution and speciation of phosphorus along a salinity gradient in intertidal marsh sediments. Biogeochemistry 45, 197–221. https://doi.org/10.1007/BF01106781.
Pant, H.K., Warman, P.R., 2000. Enzymatic hydrolysis of soil organic phosphorus by immobilized phosphatases. Biol. Fertil. Soils 30, 306–311. https://doi.org/10.1007/s003740050008.
Price, R.M., Savabi, M.R., Jolicoeur, J.L., Roy, S., 2010. Adsorption and desorption of phosphate on limestone in experiments simulating seawater intrusion. Appl. Geochem. 25, 1085–1091. https://doi.org/10.1016/j.apgeochem.2010.04.013.
Ramírez-Viga, T.K., Aguilar, R., Castillo-Argüero, S., Chiappa-Carrara, X., Guadarrama, P., Ramos-Zapata, J., 2018. Wetland plant species improve performance when inoculated with arbuscular mycorrhizal fungi: a meta-analysis of experimental pot studies. Mycorrhiza 28, 477–493. https://doi.org/10.1007/s00572-018-0839-7.
Rath, K.M., Rousk, J., 2015. Salt effects on the soil microbial decomposer community and their role in organic carbon cycling: a review. Soil Biol. Biochem. 81, 108–123. https://doi.org/10.1016/j.soilbio.2014.11.001.
Sang, Y., Jin, L., Zhu, R., Yu, X.-Y., Hu, S., Wang, B., Ruan, H., Jin, F., Lee, H., 2022. Phosphorus-solubilizing capacity of mortierella species isolated from rhizosphere soil of a poplar plantation. Microorganisms 10, 2361. https://doi.org/10.3390/microorganisms10122361.
Schoepfer, V.A., Bernhardt, E.S., Burgin, A.J., 2014. Iron clad wetlands: Soil iron-sulfur buffering determines coastal wetland response to saltwater incursion. J. Geophys. Res. Biogeosci. 119, 2209–2219. https://doi.org/10.1002/2014JG002739.
Sengupta, A., Chaudhuri, S., 1990. Vesicular arbuscular mycorrhiza (VAM) in pioneer salt marsh plants of the Ganges river delta in West Bengal (India). Plant Soil 122, 111–113. https://doi.org/10.1007/BF02851917.
Sengupta, A., Chaudhuri, S., 2002. Arbuscular mycorrhizal relations of mangrove plant community at the Ganges river estuary in India. Mycorrhiza 12, 169–174. https://doi.org/10.1007/s00572-002-0164-y.
Servais, S., Kominoski, J.S., Charles, S.P., Gaiser, E.E., Mazzei, V., Troxler, T.G., Wilson, B.J., 2019. Saltwater intrusion and soil carbon loss: Testing effects of salinity and phosphorus loading on microbial functions in experimental freshwater wetlands. Geoderma 337, 1291–1300. https://doi.org/10.1016/j.geoderma.2018.11.013.
Sparks, D.L., 1996. Methods of soil analysis. Part 3. In: Chemical methods. Sparks, D.L., Page, A.L., Helmke, P.A., Loeppert, R.H. (Eds.), The alliance of crop, soil, and environmental science societies, pp. 555–574.
Šraj-Kržič, N., Pongrac, P., Klemenc, M., Kladnik, A., Regvar, M., Gaberščik, A., 2006. Mycorrhizal colonisation in plants from intermittent aquatic habitats. Aquat. Bot. 85, 331–336. https://doi.org/10.1016/j.aquabot.2006.07.001.
Sridhar, K.R., Sudheep, N.M., 2011. The spatial distribution of fungi on decomposing woody litter in a freshwater stream, Western Ghats, India. Microb. Ecol. 61, 635–645. https://doi.org/10.1007/s00248-011-9803-1.

Tabatabai, M.A., 1994. Soil enzymes. In: Methods of soil analysis: Part 2 Microbiological and biochemical properties. Weaver, R.W., Angle, S., Bottomley, P., Bezdicek, D., Smith, S., Tabatabai, A., Wollum, A. (Eds.), Soil Science Society of America, pp. 775–833. 10.2136/sssabookser5.2.c37.

Tester, M., Smith, S.E., Smith, F.A., 1987. The phenomenon of "nonmycorrhizal" plants. Can. J. Bot. 65, 419–431. https://doi.org/10.1139/b87-051.

Tiessen, H., Moir, J.O., 2007. Characterization of available P by sequential extraction. In: Carter, M.R., Gregorich, E.G. (Eds.), Soil Sampling and Methods of Analysis. CRC Press, pp. 293–306.

Tully, K., Gedan, K., Epanchin-Niell, R., Strong, A., Bernhardt, E.S., BenDor, T., Mitchell, M., Kominoski, J., Jordan, T.E., Neubauer, S.C., 2019. The invisible flood: The chemistry, ecology, and social implications of coastal saltwater intrusion. Bioscience 69, 368–378. https://doi.org/10.1093/biosci/biz027.

Wang, Y., Qiu, Q., Yang, Z., Hu, Z., Tam, N.F.Y., Xin, G., 2010. Arbuscular mycorrhizal fungi in two mangroves in South China. Plant Soil 331, 181–191. https://doi.org/10.1007/s11104-009-0244-2.

Więski, K., Guo, H., Craft, C.B., Pennings, S.C., 2010. Ecosystem functions of tidal fresh, brackish, and salt marshes on the Georgia coast. Estuar. Coasts 33, 161–169. https://doi.org/10.1007/s12237-009-9230-4.

Wilson, B.J., Servais, S., Charles, S.P., Mazzei, V., Gaiser, E.E., Kominoski, J.S., Richards, J.H., Troxler, T.G., 2019. Phosphorus alleviation of salinity stress: effects of saltwater intrusion on an Everglades freshwater peat marsh. Ecology 100, e02672.

Woodroffe, C.D., Murray-Wallace, C.V., 2012. Sea-level rise and coastal change: the past as a guide to the future. Quat. Sci. Rev. 54, 4–11. https://doi.org/10.1016/j.quascirev.2012.05.009.

Xu, G., Shao, H., Sun, J., Chang, S., 2012. Phosphorus fractions and profile distribution in newly formed wetland soils along a salinity gradient in the Yellow River Delta in China. J. Plant Nutr. Soil Sci. 175, 721–728. https://doi.org/10.1002/jpln.201100307.

Xu, T., Veresoglou, S.D., Chen, Y., Rillig, M.C., Xiang, D., Ondřej, D., Hao, Z., Liu, L., Deng, Y., Hu, Y., Chen, W., Wang, J., He, J., Chen, B., 2016. Plant community, geographic distance and abiotic factors play different roles in predicting AMF biogeography at the regional scale in northern China: Multiple factors predict AM fungal biogeography. Environ. Microbiol. Rep. 8, 1048–1057. https://doi.org/10.1111/1758-2229.12485.

Yang, Y., Chen, L., Su, G., Liu, F., Zeng, Q., Li, R., Cha, G., Liu, C., Xing, L., Ren, X., Ding, Y., 2022. Identification and expression analysis of the lipid phosphate phosphatases gene family reveal their involvement in abiotic stress response in kiwifruit. Front. Plant Sci. 13, 942937 https://doi.org/10.3389/fpls.2022.942937.

Zhai, Z., Luo, M., Yang, Y., Liu, Y., Chen, X., Zhang, C., Huang, J., Chen, J., 2022. Trade-off between microbial carbon use efficiency and microbial phosphorus limitation under salinization in a tidal wetland. Catena 209, 105809. https://doi.org/10.1016/j.catena.2021.105809.

Zhang, Q., Sun, Q., Koide, R.T., Peng, Z., Zhou, J., Gu, X., Gao, W., Yu, M., 2014. Arbuscular mycorrhizal fungal mediation of plant-plant interactions in a marshland plant community. Sci. World J. 923610 https://doi.org/10.1155/2014/923610.

Zhao, Q., Bai, J., Zhang, G., Jia, J., Wang, W., Wang, X., 2018. Effects of water and salinity regulation measures on soil carbon sequestration in coastal wetlands of the Yellow River Delta. Geoderma 319, 219–229. https://doi.org/10.1016/j.geoderma.2017.10.058.

Zhao, G., Sheng, Y., Jiang, M., Zhou, H., Zhang, H., 2019. The biogeochemical characteristics of phosphorus in coastal sediments under high salinity and dredging conditions. Chemosphere 215, 681–692. https://doi.org/10.1016/j.chemosphere.2018.10.015.

Zhou, M., Butterbach-bahl, K., Vereecken, H., Vereecken, N., 2017. A meta-analysis of soil salinization effects on nitrogen pools, cycles and fluxes in coastal ecosystems. Glob. Change Biol. 23, 1338–1352. https://doi.org/10.1111/gcb.13430.

Zhou, J., Li, X.L., Peng, F., Li, C., Lai, C., You, Q., Xue, X., Wu, Y., Sun, Y., Zhong, H., Lambers, H., 2021. Mobilization of soil phosphate after 8 years of warming is linked to plant phosphorus-acquisition strategies in an alpine meadow on the Qinghai-Tibetan Plateau. Glob. Change Biol. 27, 6578–6591. https://doi.org/10.1111/gcb.15914.